Analysis Of Hydrogen-induced Cracking In Steel Weldments With The Lehigh Restraint Test.

ANALYSIS OF HYDROGEN-INDUCED CRACKING IN STEEL WELDMENTS WITH THE LEHIGH RESTRAINT TEST

by

Charles Gabriel Michael Interrante

A DISSERTATION

Presented to the Graduate Faculty
of Lehigh University
in Candidacy for the Degree of
Doctor of Philosophy

Lehigh University
1963

CERTIFICATE OF APPROVAL

Approved and recommended for acceptance as a dissertation in partial fulfillment of the requirements for the degree of Doctor of Philosophy.

20 Sept 1963
Date

R D Stout
Professor in Charge

Accepted, 20 Sept 1963

Special committee directing the doctoral work of Mr. Charles G. Interrante

T. F. Lukes Chairman

E. N. Kottcamp Jr.

C. W. Curtis

R D Stout

Robert S. Sprague

Acknowledgements

The author takes this opportunity to express his sincere appreciation to Dean Robert D. Stout, Professor in Charge, who contributed generously to the author's education with guidance and assistance throughout the course of this investigation. Special reference must be directed to his contributions of time, knowledge, experience, encouragement and intensity.

Appreciation is extended to the members of the author's special committee and to the chairman, Dr. Joseph F. Libsch, Head, Department of Metallurgy, for their time and suggestions.

This work was sponsored by the University Research Committee of the Welding Research Council. The continuous support, even during a time when the author suffered a protracted illness, is graciously acknowledged by the author and his family. The members of this committee must be thanked for reviewing the progress of this investigation and ensuring that special materials and equipment were available.

The author would also like to thank Bethlehem Steel Company, International Nickel Company, Linde Company, Carpenter Steel Company and the men associated with these companies who were instrumental in procuring materials donated for this investigation. The assistance of Mr. Martin Scheska, and the Machine Shop staff with the preparation of specimens and the maintenance of equipment is gratefully acknowledged. The advice and suggestions of Dr. Edward P. Beachum of the Bethlehem Steel Company are gratefully acknowledged.

ANALYSIS OF HYDROGEN-INDUCED CRACKING

IN STEEL WELDMENTS WITH THE LEHIGH

RESTRAINT TEST

Table of Contents

LIST OF TABLES

Table No.	LIST OF TABLES (Continued)	Page
19	Hardness Inspection of Weldments on ASTM A-201 at Two Heat Input Levels	94
20	Delayed Cracking Tests on Maraging Steel	96
21	Retained Austenite Measurements	97

LIST OF FIGURES

Figure No.	LIST OF FIGURES (Continued)	Page
16	Effect of Base Metal on Crack Initiation	114
17	Effect of Severity of Restraint on Crack Initiation of Low-Chemistry HY-80	115
18	Microcracks	116
19	Comparison of Carbon Equivalent Formulae Fitted to Cracking Data	117
20	Mathematical Analysis of the Manganese Factor for the Winterton Formula	118

ABSTRACT

An investigation was undertaken to define more quantitatively the major factors involved in the formation of delayed cracks in steel weldments. This investigation was particularly concerned with the role of hydrogen in delayed cracking. In addition to hydrogen, the effects of plate composition, prior base-plate microstructure, welding conditions, and the roles of martensite and austenite were studied.

The Lehigh restraint test was used to evaluate the susceptibility to delayed cracking of twelve heats of steel. Eight electrodes were used with gas metal-arc welding, and a limited number of tests were made using E-6010, E-9010, E-9015 and E-7016 coated electrodes. The gas metal-arc welding was done in atmospheres of argon containing up to 6% hydrogen in the forms of H_2 and H_2O.

An improved technique was developed to evaluate the groove relaxation associated with the onset of cracking. The device employed a differential transducer mounted across the midpoint of the welding groove immediately after welding. The signal from the transducer was fed into a multipoint recorder which permitted the evaluation of the cracking responses of many specimens simultaneously up to 30 days.

The possibility of eliminating delayed cracking by immediate postheating of the weld at low temperatures was investigated. Temperatures from 125 to 400^{o}F were studied.

The results of this investigation follow:

1. The susceptibility to delayed cracking was found to be proportional to the hydrogen content of the welding atmosphere.

2. The time required to form a crack was related by inverse functions to the hydrogen content of the welding atmosphere and the restraint level of the Lehigh restraint specimen.

3. The cracking response of low chemistry HY-80 welded with cellulosic electrodes compared almost exactly with gas metal-arc weldments made in an atmosphere of argon with 5% H_2 + 1% H_2O added. Response to delayed cracking of this steel welded with E-7016 and E-9015 electrodes was comparable with gas metal-arc weldments made in an argon atmosphere with 1% H_2O.

4. The mode of metal transfer appears to exert only a minor influence on the cracking tendencies of the steels tested.

5. Studies of the effect of prior heat treatment on the crack sensitivity of HY-80 steel revealed that resistance to delayed cracking is enhanced by a finer carbide dispersion.

6. The crack resistance of HY-80 steel was enhanced by vacuum melting, but the addition of 0.003% rare earths did not increase the resistance to cracking.

7. The critical restraint for heat affected zone cracking was found to be inversely proportional to the carbon equivalent of the base metal.

8. The electrode composition exerted only a minor influence on the susceptibility of the plate to HAZ cracking.

9. The resistance to cracking of carbon free martensite in maraging steel and the increased crack susceptibility of HY-80 with more coarse carbide dispersions suggest that carbon segregation contributes to cracking by producing regions of brittle high carbon martensite which favor cracking in the presence of hydrogen.

10. Studies on A-201 and A-212 steels indicated that delayed cracks could not be produced in the absence of martensite.

11. In general, when hardenable weld metal was deposited in low hardenability plate, the source of cracking was in the weld metal. As the hardenability of the plate increased, the cracks were transferred to the heat affected zone.

12. Postheating at temperatures typical of preheating practice was effective in eliminating delayed cracking in alloy steels. The required time at temperature depends on the size of the weld and can be reduced markedly by raising the temperature moderately.

INTRODUCTION

ANALYSIS OF HYDROGEN-INDUCED CRACKING IN STEEL WELDMENTS WITH THE LEHIGH RESTRAINT TEST

INTRODUCTION

Purpose

This investigation is concerned with the cracks in weldments involving a time delay following the welding operation. A delayed crack by definition is a crack which becomes detectable after the weldment has equalized in temperature, and is therefore, free of thermal gradients and thermal stresses. The term "cold crack" is used for cracks which occur below about 500°C (940°F). The delayed crack is a form of cold cracking, but this investigation is particularly concerned with the role of hydrogen and cracks which form below 300°F.

Delayed cracking is associated with the combined effects of the presence of hydrogen, restraint, and martensite. This investigation was undertaken to define more quantitatively the major factors involved in the formation of delayed cracks in steel weldments. Particular emphasis was placed on the role of hydrogen. The effects of plate composition, prior base-plate microstructure, welding conditions and the roles of martensite and austenite were also studied.

This type of cracking, since it does not initiate until some time after welding is most insidious. It will often be initiated after ordinary inspection procedures, and result in a catastrophic failure in service. Delayed failures, attributed to various manifestations of the hydrogen embrittlement phenomenon, have been

observed in ship plates, rotor forgings, rocket casings, steel cartridge casings, and even in giant airliners.

Hydrogen in Iron and Steel

Characteristically, hydrogen is a gas when not in solution. There is no evidence that hydrides play an important role in the behavior of hydrogen in steel. The constitution diagram is given by Zapffe[1]. Solubility increases with temperature, but it is much higher in gamma (fcc) than in alpha or delta (bcc) at a given temperature. Sieverts[2] studied the absorption of hydrogen and found that the gas dissolves atomically, and that the composition of the iron-hydrogen alloy varies with the square root of the P_{H_2}:

$$[H] = K \cdot (P_{H_2})^{1/2}$$

Zapffe[1] indicates that solubility at 1 atmosphere, expressed in cc H_2/100g Fe, decreases from 27.0 to 7.5 upon solidification at 1535°C. Solubility decreases further with decreasing temperature until the transformation to austenite at 1400°C, where it is increased from 6.0 to 9.5 At 910°C, the solubility decreases from 5.3 to 3.0 as the austenite is transformed to alpha iron. At 100°C, he gives the solubility as slightly less than 1. However, in steel, hydrogen is commonly present in amounts exceeding its solubility in iron. Also, alloy additions can raise the solubility by their effect on the amount of retained austenite.

The diffusion rate of atomic hydrogen in iron is nearly the same for single crystal and polycrystalline structures. The rapid

rate of diffusion of hydrogen atoms at room temperature is attributed to the size difference. The radius of the H^+ proton is of the order of 10^{-13} cm, while the Fe atom and the H_2 molecule are of the order of 10^{-8} cm. Diffusion of atomic hydrogen in ferrite is much faster than in austenite, being at 300°C in the former the same as at 1000°C in the latter. This is not surprising in view of the closer packing of the fcc lattice.

The driving force for diffusion is an activity gradient[3]. This activity gradient may arise from a nonuniform stress state or from a concentration-equalizing force. For stress-induced diffusion, the drift velocity of the interstitial is directly proportional to the strain gradient and the diffusion coefficient, and inversely to the absolute temperature.

$$V = \frac{D}{KT} \cdot F, \text{ where } D = D_o e^{-Q/RT}$$

V = steady state drift velocity of the interstitial

F = attracting force

D = diffusion coefficient

K = Boltzmann's constant

T = absolute temperature

D_o = a material constant

Q = activation energy

Hobson's[4] data for diffusion of hydrogen in steel fit the equation $D_\alpha = 1.82 \times 10^{-2} \; e^{\frac{-6075}{T}}$ for the range 20-110°C, equivalent to an activation energy of 12 kcal. Sykes[5], et al, give the equation

$D_\alpha = 7.6 \times 10^{-4} \; e^{\frac{-1150}{T}}$ which gives an activation energy of only 2 kcal. Others have reported values from 8 to 10 kcal for hydrogen in alpha iron. Sykes' equation for gamma iron is $D_\alpha = 1.5 \times 10^{-2} \; e^{-6000/T}$ corresponding to an activation energy of 12 kcal for gamma iron.

If the crack initiation (incubation or cracking time) is dependent upon the diffusion of hydrogen, then a plot of the log of the delay in time required to initiate a crack should vary linearly with reiprocal of the absolute temperature. Both the concentration-equalizing force and the stress-induced force are proportional to the diffusion coefficient, but since the stress-induced diffusion is related inversely to the absolute temperature, it is less sensitive to temperature changes.

Hydrogen Embrittlement

Hydrogen embrittlement is associated with a decrease in both the ultimate strength and the ductility in tension. The sustained load or stress rupture test is particularly sensitive to detection of the cracking characteristics of metals embrittled with hydrogen. Troiano[6] shows that delayed failure may occur over a wide range of applied stress, and that data taken from the sustained load type of test yield a behavior for steels embrittled with hydrogen which is a stress rupture relationship. There is an upper critical stress above which failure occurs without a time delay. Below the lower critical stress, failure does not occur. At intermediate levels of stress, failure occurs after a time delay which is shorter for higher stress.

It is well known that hydrogen embrittlement in steel is inhibited by fast strain rates and low temperatures. The loss of ductility at slow strain rates occurs only at moderate temperatures. This is in direct contrast with the conventional behavior of steels, where embrittlement is enhanced by high strain rates and low temperatures. Hydrogen embrittlement disappears at both low and high temperatures. The relatively short incubation times and the moderate temperatures at which this phenomenon has been observed suggest that the hydrogen atom is the only interstitial whose diffusion rate is large enough to explain this type of delayed failure. If hydrogen is removed prior to testing, the original ductility is restored and no embrittlement effects are detected. Hydrogen embrittlement has been observed in titanium, and titanium alloys; vanadium; columbium; and nickel, and several nickel-base alloys. Troiano[7] reports that indirect evidence indicates its presence in molybdenum and possibly tantalum.

Several theories of hydrogen embrittlement has been proposed. All investigators postulate a lattice involving defects which are termed voids, lattice rifts, Griffith cracks, or piled-up dislocations producing cracks. These voids, as they will be termed in this work, are assumed to be of large size when compared with the lattice unit cell. The localization of hydrogen is assumed to be a prerequisite to embrittlement, since very low hydrogen concentrations have been observed to cause embrittlement.

At equilibrium the concentration of hydrogen in voids is greater

than that found in the lattice. de Kazinczy[8] gives the amount of gas in ml H_2/100g Fe as $x = \frac{34.8}{(1 + 0.0006P)} \cdot \frac{Pv}{T}$, where P is the equilibrium pressure of hydrogen and v is the relative volume of cavities in percent. When the hydrogen pressure in the cavities is not the equilibrium value, hydrogen will diffuse to or from the void. During plastic deformation, dislocations may collect hydrogen by migrating past a region rich in hydrogen.

In the theories of hydrogen embrittlement, the postulated mechanisms depend upon whether the hydrogen assumed to be embrittling is in the void, at the surface of the void, or in the region of the most severe triaxial stress state around the void. In the case where the hydrogen in metal under the most severe triaxial state is assumed to be damaging, the void acts like a notch to increase the stress placed on the metal around the void, where hydrogen in solution causes embrittlement.

Historically, Zapffe, et al[9,10] first explained hydrogen embrittlement with the planar pressure theory. They postulated that atomic hydrogen precipitates into voids and forms molecular hydrogen which builds up sufficient pressure to cause premature fracture. Strain enlarges the voids and further precipitation of hydrogen is required to maintain a damaging pressure. Sims[11] advanced a variation on this theory, the slip plane theory. Hydrogen is assumed to precipitate in slip planes under very high pressure to cause lattice distortions. Another variation in the planar pressure theory was introduced by Bastien and Azou[12]. It differs in the mechanism of

delivery of hydrogen to the voids, suggesting that hydrogen is concentrated around dislocations as a Cottrell atmosphere. Under strain, as a dislocation moves through the lattice, the dislocation is presumed to discharge a certain amount of hydrogen when it reaches a void. Still another variation of the pressure theory was advanced by de Kazinczy[13] in the expansion energy theory. This theory is based on the thermodynamic concept that an expanding gas is accompanied by the release of energy. In his viewpoint, the void is filled with an equilibrium hydrogen pressure. The hydrogen gas in the void releases energy which is added to the released strain energy during crack growth, thereby lowering the applied stress necessary for crack growth. These theories have all been based upon the assumption that the damaging hydrogen is in the voids.

Petch and Stables[14] assumed the hydrogen on the surface of the void to be damaging. They suggested that the adsorption of hydrogen on the surface of a crack, formed from an array of dislocations piled up against a grain boundary, is responsible for lowering the stress required for fracture by lowering surface energy.

Morlet, Johnson and Troiano[6,7,15,16] have advanced the triaxial stress theory which assumes that hydrogen in solution near a void causes embrittlement. Their work appears to disprove both the surface adsorption theory and the planar pressure theory, and they indicate that a satisfactory theory of hydrogen embrittlement may have to await the development of a general theory of fracture. This theory predicts that at the region of maximum triaxial stress in the lattice near a

void or stress raiser, a concentration of hydrogen in solution will be found which exceeds that found in the surroundings at equilibrium. Hydrogen in the void is non-damaging. A critical amount of stress is required to cause a critical or damaging concentration of hydrogen. Less than this amount of stress will cause some segregation but not the concentration of hydrogen corresponding to the critical amount.

The diffusion of hydrogen into this region is induced by the stress gradient created by the region of triaxial stress. To evaluate the hydrogen segregation in dilute solutions, the equilibrium distribution of hydrogen atoms was described[17] in terms of a Boltzmann distribution function.

$$C = C_o e^{-U/KT}, \text{ where}$$

C = interstitial concentration at any point,

C_o = average interstitial content,

U = interaction energy between the interstitial and the stress field,

K = Boltzmann's constant, and

T = absolute temperature.

When the concentration (C) reaches the critical hydrogen concentration (C_c) in the position of maximum triaxial stress, the initiation of a crack occurs. The crack is propogated by the same mechanism, after hydrogen diffuses to the triaxiality region ahead of the crack. Crack propogation is therefore, discontinuous. At high temperatures, the strain-induced concentrating force is balanced by the clasical concentration-homogenizing force, and embrittlement is less pronounced

or inhibited completely. At low temperatures cracking is retarded or inhibited completely, because the hydrogen diffusion rate decreases as the temperature is lowered.

Cold Cracking in Weldments

Several comprehensive reviews of cold cracking in weldments have been given in the literature[18,19,20]. Also, a bibliography has been prepared on the effects of hydrogen embrittlement[21]. The problem of cold cracking is complex and many investigations have been made in this area over the past thirty years. An attempt will be made here to cite only a few of the important observations, and some of the principles developed through the years. The term "cold cracking from hydrogen embrittlement" or "delayed cracking from hydrogen" would approximately describe this form of cracking, but many misleading names have been used to describe the phenomenon. Among these are included the names "underbead cracking", and "cold cracking in the heat affected zone". Both of these are misleading. "Underbead cracking" only refers to a location which is common among other kinds of parent metal cracking, and "cold cracking in the heat affected zone" rules out the possibility of cracks forming or initiating in the weld metal. For brevity, the terms "delayed or cold cracking" will be used here.

All steels undergoing the austenite-martensite transformation at room temperature seem to be sensitive to cold cracking. It appears that this may include mild steels, low alloy steels, high tensile steels and high carbon steels. So microcracking might be considered as a definite possibility for nearly all steels except very mild steels and

austenitic steels.

The hard and often brittle structure of untempered martensite formed in the HAZ with severe cooling conditions is generally associated with the cracking phenomena in the sensitive steels. The crack susceptibility of this structure is attributed to the low gas permeability and lack of ductility of the lattice.

The cooling rate effects the susceptibility to cold cracking. The rate of cooling at high temperatures (1300°F) determines the transformation products to be found in the HAZ, whereas the rate of cooling at low temperatures (400°F) probably controls the progress of delayed transformation. The most significant temperature at which the cooling rate in the HAZ appears to exert a major influence on the initiation of the cracking seems to be 570°F, at least for the Mn-Mo steels investigated at the BWRA. Of course, faster cooling rates create the undesirable conditions which lead to delayed cracking. Preheating has been shown to be an effective means of reducing the cooling rate and the susceptibility of steels to delayed cracking.

Hydrogen is introduced into weldments because the welding arc is capable of dissociating hydrogen gas and hydrogen bearing compounds and the molten weld metal has a high occlusive capacity for atomic hydrogen, which increases for higher H-potentials. The H-potential is a qualitative measure of the proportion of hydrogen in the welding atmosphere which will tend to dissolve in the molten metal during a given reaction. Water vapor, air and pure hydrogen gas are the normal sources for introducing hydrogen into the weld

puddle.

The literature gives evidence of both inter- and trans-crystalline crack (or microcrack) paths[18,19]. In the weld metal, cracks running indifferently between and through the dendrites have been shown[18]. This is in complete agreement with the theory, which indicates no preference to the grain boundaries.

Carbon Equivalent

Heat affected zone cracking, resulting from welding, is dependent on the hardenability of the steel being welded. Since hardenability is dependent on composition, attempts have been made to relate weldability, in terms of heat-affected zone cracking, to composition by calculating the equivalent carbon content. If the carbon equivalent exceeds a certain critical level, it is assumed that the steel cannot be welded unless special precautions are taken.

An early formula used to evaluate weldability was

(1)
$$C.\ E. = C\% + \frac{Mn\%}{6}\ .$$

This formula is taken from a more complex formula presented by Dearden and O'Neill[22]. From an analysis of weldability test results at Battelle Institute, Voldrich, Martin and Hareler[23] gave the following formulae:

(2)
$$C.\ E. = C\% + \frac{Mn\%}{4} \quad \text{and}$$

(3)
$$C.\ E. = C\% + \frac{Mn\%}{4} + \frac{Si\%}{4}\ .$$

Formula (3) has been widely used by several authorities including Stout and Doty[24]. Winterton[25] presents a formula for alloy steels based on the end of the martensite transformation temperature (M_f) in the austenite to martensite transformation.

(4)
$$C.\ E. = C\% + \frac{Mn\%}{6} + \frac{Ni\%}{20} + \frac{Cr\%}{10} - \frac{Mo\%}{50} - \frac{V\%}{10} + \frac{Cu\%}{40}$$

It should be noted that formulas utilizing hardness, ductility, and the amount of cracking in the heat-affected zone have also been used to evaluate weldability. The following formula[25] is an approximation, relating the Vickers diamond pyramid hardness and the carbon equivalent.

(5)
$$D.\ P.\ H. = 1200\ (C.\ E.) - 200$$

A maximum D. P. H. value of 350 is given as the limit for hardness in the heat-affected zone to avoid cracking. It must be remembered that this is only a first approximation, since even a mild steel[19] may exhibit sensitivity to cracking.

Heuschkel[26] used formula (6) to evaluate weldability in the T-bend test. In this test, the welded fillets were stressed in tension. His formula follows:

(6)
$$C.\ E.\ (70^{o}F) = C\% + \frac{Mn\%}{10} + \frac{Si\%}{9} + \frac{Ni\%}{99} + \frac{Cr\%}{10} + \frac{Mo\%}{3} + \frac{V\%}{6} + \frac{Cu\%}{99} + \frac{P\%}{1.4}.$$

He found that the results were temperature dependent and the above formula is valid only at $70^{o}F$.

EXPERIMENTAL PROCEDURE

EXPERIMENTAL PROCEDURE

Materials and Welding Apparatus

Lehigh restraint test specimens were prepared from the twelve heats of steel whose chemical compositions are listed in Table 1. Table 2 gives heat treating temperatures and the letter code designation used in numbering specimens. All steels were tested as 1" plate except code HH which was 1-1/2". Microstructures are shown in Figures 1 and 2. All heat treatments were performed prior to machining the welding groove and restraint slits. The single exception was the 18% Ni maraging steel which was too hard to machine readily in the maraged condition. These specimens were machined in the annealed condition. Prior to welding, the oxides formed during maraging were removed from the groove and slit areas with wire brushes and emery cloth.

Eight electrodes were used with the shielded-inert-gas-metal-arc (SIGMA) process. Their compositions are given in Table 3. Also, a limited number of welds were made with E-6010, E-9010, E-7016 and E-9015 stick electrodes. All electrodes were from commercial heats except the pure iron and Alloy Nos. 1 and 3. The pure iron electrode was prepared by Carpenter Steel Company as a 15 lb. laboratory heat. The two alloy electrodes were experimental heats prepared by the Linde Company.

Welding Technique

An automatic shielded-inert-gas-metal-arc apparatus was used. Current was supplied by a 3 phase rectifier unit. The test specimen was securely fastened to the welding bed with quick release clamps shown in Figure 3A. With this clamping arrangement, the restraint specimen was welded without arc blow. Some tests were made with 3/16" diameter coated electrodes. All welds were made with automatically controlled travel speeds.

The welding bed was fitted for bottom purging the welding groove with a flow rate of 7cfh. Gas flow rates from the SIGMA torch were 50cfh, shield, and 5cfh purge. All welds were made using reversed polarity to obtain spray transfer at 250 amperes, 32 volts, and a travel speed of 15"/minute, except as noted in the tables listing cracking responses.

Prior to welding, the grooves were degreased with acetone. A small ball of degreased steel wool placed into the groove at the start of the bead ensured proper initiation of the arc. On specimens using a double pass, the second pass was made after a 2-1/2 minute delay. During this time, the surface of the first bead was wire brushed to remove oxides. The Appendix gives actual readings.

In an attempt to maintain reproducible conditions, the amount of hydrogen or water introduced into the welds from the electrodes was minimized by storing electrodes in cans containing a desiccant and by baking the electrodes for 1-1/2 hours in an oven at 190±10°F. Welds were made 1 to 3 hours after removal of the wire from the baking oven.

Coated electrodes were used immediately after being removed from the oven. The high hydrogen cellulose electrodes were baked for at least 24 hours at 150°F, and the low hydrogen electrodes were stored at 450°F.

Lehigh Restraint Test

The Lehigh restraint test was used exclusively to evaluate cracking responses in this investigation. This test was developed by Stout, Tor, McGeady and Doan[27,28] who used it to evaluate quantitatively cracking in steel weldments. Until recently, the test had not been used in any investigation of delayed cracking. However, Agnew[29] reported cracks that occurred in E-6010 weld metal with delay times up to 4 hours after depositing at sub-zero temperatures. Beachum[30,31] used the test to evaluate the susceptibility to delayed cracking of four base metal compositions welded with four electrodes in hydrogen bearing atmospheres. The success of Beachum's work with the Lehigh restraint test prompted the Welding Research Council to sponsor the present investigation.

The Lehigh restraint specimen shown as Figure 4 derives its name from the following considerations. When molten weld metal freezes onto a relatively cold base plate, the weld metal contracts a greater amount than the base metal because the weld metal is cooling through a broader temperature range during the time required for the weld metal and base metal to equalize in temperature. This differential contraction creates tensile forces in the weld and heat-affected zone areas, because they are restrained by the base metal from contracting freely. This restraint is offered by the two beams supporting the sides of the welding groove in the Lehigh restraint specimen. Since these beams are continuous at the ends of the groove, the major axis of loading is transverse to the longitudinal axis of the groove.

The restraint is imposed solely as the result of the thermal cycle of welding.

The magnitude of the load imposed on the weld is a function of the beam deflection. Since the base plate is both lower in temperature and significantly greater in cross section than the weld metal, the latter must supply the major portion of the strain. Plastic adjustments are made by the weld metal. Therefore, the deflections experienced by the beams of the base metal are within the elastic region. The deflection is inversely proportional to Young's Modulus, which is essentially the same for all steels. Therefore, the degree of restraint offered by the specimen is not changed by changing the strength of the base metal. The beams can be finned, as shown in Figure 4, to decrease the effective thickness of each of the beams, and thereby decrease the restraint without changing the cooling rate. The degree of restraint is specified in inches by the distance X for plates using the standard 5 inch groove. Normally, X is varied in 1/2 inch intervals from 2-1/2 to 8 inches of restraint.

If the full 8 inches of restraint offered by the specimen with the 5 inch groove prove to be insufficient, a higher restraint is obtained by depositing a 3" bead on the standard 5" groove. When this is done, the 5" groove is machined into the specimen and 1/2 inch holes are drilled (3-1/2" between centers) to provide a 3" land, centered on the 5" groove. This level of restraint is more severe than that provided by the 5" bead because the average unit stress in the weld and HAZ metal is inversely proportional to the area supporting the transverse

load. Also, the cooling rate is more severe for the 3 inch bead. This restraint level is designated "3 inch bead".

The standard groove length of 5 inches can be shortened to 3 inches to decrease the length of the beams and thereby increase the restraint offered by the specimen. This level is more severe than the 3" bead on a 5" groove. It is designated "3 inch groove".

The maximum restraint which can be applied without producing a crack of size greater than the critical crack (defined under Crack Detection) is called the critical restraint. Thus, the test is used quantitatively to evaluate the crack sensitivity of steels by determinations of the effect of selected variables on the critical restraint.

In this investigation the standard procedure was used, one factor being varied at a time. Stout[27,28] classified the test variables as "external factors" and "internal factors". The "external factors" are those which can be directly controlled such as welding atmosphere; plate composition, thickness and temperature; groove geometry; electrode composition and diameter; heat input; etc. "The internal factors" can be controlled only indirectly. These include cooling rate, penetration, and composition of the fused weld metal. "Inherent factors are those that are beyond experimental control such as allotropic transformations, diffusivity, and physical properties of the weld. In this investigation, every effort was made to maintain reproducible conditions so that the effect of individually varying each of the selected "external factors" could be properly evaluated.

Crack Detection

Beachum[30,31] found that the delay time required to form a crack in the Lehigh restraint specimen could be evaluated with a timer connected to a sensitive microswitch mounted across the welding groove. The formation of a delayed crack was thus found to be associated with a groove relaxation of 0.003" to 0.020" and delay times ranging from minutes to days from the time of welding.

For the present investigation, an improved technique was developed to observe the formation of delayed cracks. A linear-variable differential-transformer type of transducer was mounted across the midpoint of the welding groove immediately after welding. On one side of the groove, the transducer is attached using a brass mount fitted into a hole in the plate adjacent to the midpoint of the groove in the test specimen. See Figures 3B and 5.

The core, inside the transducer, is spring loaded against a brass bar similarly attached to the opposite side of the weld groove. This mount is fitted with an adjustment screw which permits setting the pointer at the desired position on the recorder chart used to detect the crack. The voltage input to the transducer is regulated at 25V±1% to assure stability. The output from the transducer is rectified, filtered, and fed into a multipoint recorder through a switchboard as depicted in Figures 6 and 7. The crack is detected when the relaxation across the weld bead changes the position of the core inside of the transducer. This changes the output voltage of each of the secondary windings.

The voltage output is directly transmitted to the chart on the recorder where it can be measured in terms of thousandths of an inch of relaxation across the groove. The instrument was calibrated and found sensitive to 0.0001 inch expansion or contraction. The system can be converted readily to provide increased or decreased sensitivities. The behaviors of six specimens were recorded simultaneously on the apparatus shown in Figure 3c.

Only specimens with cracks greater than 1/16" length measured on a macroscale in the transverse section were considered cracked, and this was defined as the critical crack length. For this determination, the metallographic section corresponding to the dotted line in Figure 4 was removed and examined macroscopically for cracks after polishing and etching. These cracks originated at the highly stressed notch area at the root of the bead. A crack 1/16" in length gave a relaxation of 0.002" when measured by the transducer-recorder system described.

Beachum found that after 15 minutes from the time of welding, the temperatures of the bead and the plate were equalized in the Lehigh restraint specimen when a heat input of 34 kilojoules per inch is used. Thus, 15 minutes was the criteria used as the lower time limit for delayed cracks. A crack forming prior to this time could have been caused by thermal effects, so it would not be considered delayed.

Hydrogen in Weldments

To study the effects of hydrogen in SIGMA weldments, two different sources of hydrogen were employed:

(1) Mixtures of hydrogen gas and 99.95% purity argon gas were used for both purge and shield gases. Purity of the hydrogen gas was reported as follows:

99.8% (min) H_2,

0.048% (max) O_2,

0.09% (max) N_2, dew point (-75°F)

(2) Argon gas (99.95% purity) was bubbled through water at room temperature. The argon picked up about 1% water vapor by this technique. The dew point of argon "wet" by this technique was 9.7± 0.9°C. This corresponds to 1.2±06% water vapor in argon.

To compare the amounts of diffusible hydrogen introduced into various types of weldments, the hydrogen evolution apparatus (Figure 3D) described by Beachum[30,31] was used. These determinations were made under mineral oil. To minimize loss of diffusible hydrogen to the mineral oil, the oil bath was saturated with hydrogen prior to testing and maintained at a temperature of 90°F with several cc's of hydrogen in each tube. Some investigators[32] have preferred mercury to mineral oil. Measurements of this kind are only relative because the bath, open to the air, will transport and lose some of the hydrogen to the atmosphere. The dimensions of the specimen for this study were 1" x 1" x 5-1/2".

It was the aim to prepare specimens in the most reproducible

manner, which would permit rapid cooling prior to transferring the specimen at room temperature to the mineral oil bath for the 72 hour evolution analysis. Copper chill plates 3/4" x 3-1/2" x 12" were employed adjacent to the test specimen. A five inch deposit was used for each run. To accelerate cooling, specimens were removed from the jig and quenched in water. After the specimen reached about 100°F, it was transferred from the water to an ethyl alcohol bath to facilitate drying before placing it under the mineral oil bath. The total time elapsed from welding to placing the specimen under the oil bath was 1-1/2 to 2 minutes.

Derge, et al[33,34] have divided the loss of hydrogen from steel into two parts: "diffusible", which can be removed in a practically measurable time, and "non-diffusible" which is the residual amount. Since the evolution apparatus evaluated only that hydrogen which diffuses from the specimen at 90°F under a 12" column of mineral oil, a separate study was employed to evaluate the residual hydrogen. This non-diffusible or residual hydrogen was evaluated by hot extraction at 1150°F for 60 minutes. These analyses were performed at the Bethlehem Steel Company laboratories. The specimen thickness was reduced to 3/8" for these determinations so that the vacuum extraction apparatus could accomodate them.

Postheating Studies

If delayed cracking is affected by the diffusion of hydrogen, then the temperature of the weld and base metal after welding should be among the most important variables affecting the cracking tendency of steels. Several temperatures were selected to study this variable: 0°F, 80°F, 125°F, 150°F, 200°F, 300°F, and 400°F. The procedure used for the 0°F specimens was as follows:

1. The microformer was attached immediately after welding.
2. A 150°F tempilstik was used to determine the time at which the weld had equalized in temperature with the base plate. This took about 12 minutes.
3. After the specimen had equalized in temperature, it was placed into a bath of dry ice in alcohol cooled to -15°F.
4. The bath temperature was then maintained at 0°F with the specimen submerged until it had equalized with the bath (about 15 minutes).
5. The specimen was then transferred from the alcohol bath to an electric freezer, preset and controlled at 0°F, from which the cracking response was monitored on the multipoint recorder.

Specimens postheated above room temperature were placed in an oven five minutes after welding. Immediately after welding, the microformer had been attached to the specimen and set for recording. The oven technique produced slow heating rates in the test specimen. Faster heating rates were obtained by using 1000 and/or 1500 watt resistance strip heaters, shown in Figure 3E, on both sides of the welding groove, as shown in Figure3F.

Retained Austenite Determinations

For this investigation it was necessary to find a quantitative method of determining the percentage of retained austenite in small areas from sections of weldments. The specimen size was of the order of 1 to 2 cm^2 with the amount of retained austenite ranging downward from 3 percent in hardened steels. Since it was desired to detect any decrease in the percentage of austenite occurring in a short time span, the technique selected had to be both accurate and rapid. Specimen preparation time was also quite limited, since the anticipated time during which most of the transformation would likely occur would be within two hours from the time of welding.

Methods of detecting retained austenite include metallographic, dilatometric, magnetic, and x-ray techniques. The only technique which even approaches the above requirements is the internal standard method of x-ray diffraction developed by Averbach and Cohen[35]. This method is not only satisfactory for hardened steels, but it may be employed when a third phase is present in significant proportions.

For this method, the martensite, which coexists with austenite, was used as the internal standard. The intensity of an austenite diffraction peak is a continuous function of the percentage of austenite in the specimen. The integrated intensity of radiation of one or more of the austenite peaks was compared with the integrated intensity of radiation from one or more of the martensite peaks. The mathematical calculations are described by Cullity[36], and Bierwirth[37] gives tables to simplify calculations. If a diffractometer is used

with a pulse-height discriminator and the proper choice of radiation, the background radiation can be reduced to a very low level, an accurate quantitative determination can be made in a matter of minutes.

For this investigation on a Siemens x-ray diffractometer was employed using molybdenum radiation at 50 kV and 14 mA. A special beam collumator was designed for this work to increase the intensity of the beam so that determinations could be made on small areas. Pulse height discrimination was used to select only the characteristic K_{α} radiation. This greatly reduced the background and permitted the determination of less than 1% austenite with an estimated accuracy of less than ± 0.2 percent.

Special care was taken in preparing the specimens used for these determinations, since austenite transformation may result from mechanical working if care is not taken. A wet grinding belt was used with very light pressure to prepare a smooth flat surface for the diffractometer. A special specimen holder was designed to accomodate the smaller specimens in the diffractometer.

RESULTS AND DISCUSSION

RESULTS AND DISCUSSION

Hydrogen Contents of Weldments

The data presented in Table 4 can be used to compare the relative amounts of diffusible hydrogen introduced into steel by the water or hydrogen-bearing argon atmospheres, and the atmospheres of low or high hydrogen coated electrodes. The cellulosic electrodes gave up on the average 3 cc's H_2 per 5 inch weld. The low hydrogen electrodes, however, yielded only 0.1 cc's H_2 per 5 inch weld. The specimens welded with an argon atmosphere containing 1% H_2O yielded less diffusible hydrogen on the average than that given up by the low hydrogen electrodes. However, the atmosphere of 5% H_2 + 1% H_2O gave 0.3 cc's H_2 per 5 inch weld. No evolution could be detected from specimens welded with a dry argon atmosphere.

Table 5 compares the diffusible, residual and total hydrogen contents of weldments made with an argon atmosphere bearing 10% hydrogen, and a dry argon atmosphere to which no hydrogen was added. Specimens 1 and 2 were welded with 10% H_2 in the argon atmosphere, quenched immediately after welding, and stored in liquid nitrogen until hot extraction measurements were performed. They yielded about 1 cc H_2 per inch of weld. If the specimen is held at 95°F for 72 hours in the evolution apparatus before performing the hot extraction determination, one detects only about half as much hydrogen per inch of weld. The data suggest that much of the diffusible hydrogen evolved is not detected in the evolution apparatus. Thus, it must be remembered that the diffusible

hydrogen determinations are only relative and not absolute.

When dry argon is used for the shield gas, no hydrogen is detected evolving from the specimen at 95°F under mineral oil. The residual hydrogen determination of specimens welded with the dry argon revealed that the welded specimen contained less hydrogen than the unwelded base metal. Thus, the heating cycle will remove hydrogen from the base metal if care is taken to keep the welding atmosphere dry and free from hydrogen.

For commercial welding of steel plates which are susceptible to delayed or hydrogen cracking, it would be desirable to know the hydrogen content of the weld metal or of the base metal which would cause cracking under a given set of welding conditions. This problem is one which is not readily resolved. Experimental evidence obtained in this investigation points out that this threshold level required to cause cracking will vary for different steels, heat treatments, restraints imposed, welding conditions, and atmospheres.

Experimental evidence[15,16] has indicated that hydrogen in steel exists in two forms. The hydrogen found in steel plates apparently is innocuous in the as-rolled or heat treated plates, even though the amount of hydrogen may be relatively large. However, the addition, by cathodic charging, of an amount of hydrogen which is too small to measure with currently available techniques, can cause embrittlement in some steels.

If the specimen is "charged" with hydrogen and allowed to remain at room temperature for as little as 30 minutes before performing a

hydrogen determination, the specimen will lose a great portion of the hydrogen during this 30 minutes. Furthermore, in preparing a specimen for a hydrogen determination, the act of removing a sample of metal from a large plate introduces heat which accelerates the rate of escape of hydrogen.

When hydrogen is introduced as a super-saturated solution into the weld bead through the welding atmosphere, it will diffuse both into the base metal through the underbead area and to the atmosphere through any open surface. Diffusion of hydrogen atoms into the depleted areas will occur until the system reaches equilibrium and the concentrations are the same in bead and base metal. Thus, the hydrogen content of the underbead area changes with time after welding. It is a function of the hydrogen contents of the base metal and the weld metal just after solidification of the bead.

Sieverts[2] measured the solubility of hydrogen in iron at 1 atm for a range of temperatures. The valve found in Table 5 of 18.2 cc's total H_2, evolved from bead and base metal per 100 grams of bead deposited, is about midway between the solubility limits for iron at 1535°C. Sieverts reports the solid state solubility as 13.4 cc's/100g Fe and for the liquid state 26.7 cc's/100g Fe. This indicates either that hydrogen is trapped in a non-equilibrium state in the weld metal upon solidification, or that hydrogen is transferred rapidly at elevated temperatures from the liquid weld metal to the heat affected zone before, or shortly after, solidification of the weld metal occurs. Further, the contents indicated for a 100 gram

section of bead and base metal represent the hydrogen concentration if it were considered to be uniformly distributed throughout the bead and base metal. These data show that the content after welding in the atmosphere of argon plus 10% H_2 is more than double the 0.8 ppm found in the base metal prior to making the deposit, whereas, in the specimen welded with the dry argon atmosphere, the hydrogen content was reduced by a factor of 2 to 3. Therefore, it is anticipated that the hydrogen concentration of the heat-affected zone will be at least doubled at some time after welding while hydrogen atoms diffuse to the base metal after welding in an atmosphere of argon with 1% H_2O. It is also expected that the hydrogen concentration will be diminished considerably in the underbead area when the dry argon atmosphere is used, but with time it should approach the level found in the base metal.

Crack Susceptibility Affected by Hydrogen Content of the Welding Atmosphere

Gas-metal arc weldments

The critical restraint levels were determined for low chemistry HY-80 steel welded with Alloy No. 2 electrode in atmospheres of various hydrogen contents. These data are presented in Table 6. With the dry argon atmosphere, cracks were not produced in the Lehigh restraint specimen. Eight inches of restraint produced a crack in 2.3 hours after welding in an atmosphere containing 1% H_2O. With 5% H_2 in the atmosphere, a crack could be initiated in a specimen of 6 inches restraint in 1.5 hours, and only 0.7 hours were required at 6 inches for the specimen welded in the atmosphere containing 5% H_2 + 1% H_2O. Thus, the susceptibility to delayed cracking was found to be proportional to hydrogen content of the welding atmosphere, and the amount of hydrogen in free or combined form appear to act in a cumulative manner in the range of concentrations from 0 to 6% hydrogen, as depicted in Figure 8.

The data for the three series of tests presented as Figure 9 reveal that the delay in time required to cause cracking is proportional to the reciprocal of the restraint level provided in the Lehigh restraint test. At low hydrogen contents, higher restraint is required to initiate cracking in the Lehigh restraint test. Note that the slope of the A-302 line dictates that, at least for the bead size studied (34 kji), long time cracking becomes virtually impossible for conditions of severe crack susceptibility. Similarly, Figure 10 shows

that for a given restraint level, the time required to initiate a crack diminishes as the hydrogen content increases. Thus, both the restraint level required to cause cracking and the time delay required to initiate a crack are inverse functions of the hydrogen content of the welding atmosphere in the range 0 to 6% hydrogen.

Note in Table 6 and Figure 8 that at the restraint level just above the critical restraint, at lower hydrogen contents, cracks were detected at longer times, but the maximum time to crack was diminished as the hydrogen content was increased. As a first approximation, this observation was used to shorten the number of test specimens required to determine the critical restraint.

Coated Electrode Compared With Gas-Metal Arc Weldments

A comparison of the crack susceptibilities of weldments made in the atmospheres of the coated electrodes and atmospheres of argon with various hydrogen contents is depicted in Table 7. The high hydrogen electrodes E-XX10 cracked at a level of 5-1/2" to 6" restraint with no apparent dependence on either the prior heat treatment of the base metal or the strength level of the electrode. The cracking response for these electrodes compared almost exactly with that obtained with the alloy electrode using 5% H_2 + 1% H_2O in the welding atmosphere.

The amount of diffusible hydrogen measured from the E-XX10 series was about 10 times the 0.3 cc's / 5 inch weld which evolved from the welds made with the argon with 5% H_2 + 1% H_2O. Since the

cracking responses were so similar, it appears that increasing amounts of hydrogen in the welding atmosphere can cause the crack susceptibility to increase, but this effect may have a limit which is near the 5% H_2 + 1% H_2O (or 6% H_2) level. Figure 8 indicates this trend for HY-80.

The atmosphere from low hydrogen electrodes compared very favorably with the SIGMA atmosphere of 1% H_2O in argon. Both atmospheres produced cracking responses at times of about 2 hours in the 8 inch specimen. The annealed base metal was more crack sensitive than the normalized plate with both atmospheres tested. The effect of prior structure was more pronounced for the specimens welded with the alloy electrode in the argon + 1% H_2O atmosphere.

In summary, the strength level of the electrode had no effect on delayed cracking response for strength levels of 60 to 90 ksi. Increasing the hydrogen content from zero to 6% of the welding atmosphere decreases the resistance to delayed cracking, and concentrations much greater than this did not decrease the resistance to cracking further. The annealed base metal was more susceptible to delayed cracking than the normalized base plate when welded in atmospheres of relatively low concentrations of hydrogen. At high concentrations of hydrogen, no difference was detected in cracking response due to the prior heat treatment of the base metal.

Cracking Response of Single vs. Double Pass Welds

Double pass welds were compared with single pass welds by making weld metal deposits in both "dry" and "wet" argon atmospheres. The data are presented as Table 8. The "wet" argon contained about 1% H_2O and the "dry" argon had been passed through a large tank of desiccant. The single pass weld deposited in the "dry" argon atmosphere did not crack even at the highest restraint level. The "wet" argon atmosphere introduced enough hydrogen into the single pass weldment to cause cracking at the 6 inch restraint level in 2.5 hours. When two passes of "wet" argon were deposited, cracking occurred at an even lower restraint level. At 5 inches of restraint, a crack formed in 7.0 hours. When a "wet" pass was deposited and followed by a "dry" pass, cracking occurred at the same level as the single pass "wet", but only after a time delay of 48 hours. Since this indicated that only a slight reduction in restraint would be required to stop cracking, a duplicate specimen was prepared, and it did not crack. When a "dry" pass was deposited and followed by a "wet" pass, cracking was inhibited up to the 8 inch restraint level where a crack formed in 6.5 hours. To interpret these results, one must examine the factors affecting the hydrogen content of the highly stressed heat affected zone regions near the root of the notch where cracks are initiated. A review of some of the pertinent data will be given as verification of the analysis.

Table 5 shows that welds made in a hydrogen-bearing atmosphere will have a higher hydrogen content than the original content of the base metal, and weldments deposited in a "dry" argon atmosphere will

have a lower hydrogen content than the content of the base metal prior to welding.

Since cracking does not occur immediately after the weldment has cooled to temperatures at which it contains much more hydrogen than its solubility would dictate, it must be concluded that the concentration of hydrogen is a function of time in the areas wherein cracking is initiated. Troiano[6] has shown that the concentration of hydrogen will increase with time in the area of maximum triaxial stress. At equilibrium, the highly stressed region would have a greater concentration than that of the surrounding metal. When a bead is deposited in a hydrogen-bearing atmosphere, high concentrations of hydrogen are dissolved in the molten pool. Upon solidification and during cooling, the solubility of hydrogen is reduced drastically. During the welding cycle, the heat-affected zone is subjected to temperatures at which the diffusion of hydrogen is greatly accelerated. Although the time at elevated temperatures is limited by the nature of the welding cycle, it is reasonable to assume that it is of sufficient duration for the heat affected zone metal near the fusion line to have a hydrogen concentration which is almost equal to that found in the weld metal. The plate temperature becomes uniform after 10 to 15 minutes from the time of welding. It is from this point in time with which we are concerned in an investigation of delayed cracking. It will be assumed that the bead and the heat affected zone near the fusion line in the area of the notch, where cracks initiate, have a uniform hydrogen content.

Depicted in Figure 11-A is the situation wherein the bead and the

heat affected zone at 10 minutes after welding are charged with a concentration $(H)_2$, while the concentration of the surrounding base metal is $(H)_1$, which is equal to that of the remainder of the base metal. The charged weldment will outgas to the atmosphere in an attempt to attain equilibrium. The highly stressed regions, however, have an affinity for hydrogen, and at equilibrium the concentration in these regions is greater than that found in the surrounding metal. Competing with the increase in hydrogen concentration at the highly stressed areas is the logarithmic decrease in concentration of the surrounding base metal associated with outgassing. This relationship is depicted in Figure 11-B. This figure also shows the anticipated changes in concentration in the highly stressed regions. This curve exhibits a maximum which corresponds to a concentration greater than that which was found in the highly stressed regions immediately after welding. As time proceeds, the concentration in these regions is degreasing until outgassing has ceased. At this time the equilibrium concentration exceeds the concentration in the surrounding areas. In Figure 11-C, the effects of a single "wet" pass are compared with the effects of a single "dry" pass. The "dry" pass exhibits a minimum immediately after welding, and with time, the concentration increases until it reaches the equilibrium value, a function of the concentration in the surrounding base metal. The increase is due to the combined effects of a hydrogen-concentration-equalizing force, causing diffusion from the base plate into the depleted regions and the stress-induced affinity for hydrogen of the highly stressed regions.

A crack will initiate if the hydrogen concentration reaches a critical level. This crack propagates if the critical level is maintained in the triaxiality region. Higher restraints serve to increase the stress-induced force, causing both the rate of diffusion and the equilibrium concentration of hydrogen to increase. A higher hydrogen content in the base metal produces a critical level of hydrogen in shorter times simply because the diffusion path is decreased and lower restraints will be sufficient to produce the critical hydrogen level.

The following data are submitted in support of this analysis. Figure 8 shows that the crack susceptibility is a function of the hydrogen content of the welding atmosphere, and Figure 9 shows that the cracking time is proportional to the reciprocal of the restraint level provided in the Lehigh restraint specimen. At a given level of restraint, a particular minimum concentration of hydrogen seems to be required to cause cracking with a given weld metal-base metal combination. Figure 10 shows that for a given restraint level the time required to initiate cracking decreases as the hydrogen content increases.

This analysis should be capable of explaining the results of the double pass restraint tests. The second pass of a two pass weld will present a barrier in the escape path of the hydrogen of the first pass. In the "wet" - "wet" series of tests, this means that the charged bead on the bottom near the notch has an excess concentration of hydrogen, the escape of which is inhibited because there is a charged bead between the first bead and the atmosphere to which hydrogen must escape to

avoid cracking. Consequently, the critical restraint level is lower for the "wet" - "wet" double pass than for the "wet" single pass. When a "dry" pass was deposited after having deposited a "wet" pass, the sensitivity to cracking was somewhat diminished. This is not surprising since the "dry" pass was found to reduce the concentration of hydrogen in the "wet" pass to inhibit cracking. When the "dry" pass was deposited first, however, the "wet" pass is not physically near to the notch area of high stress at the root of the bead where cracks initiate. This means that the hydrogen must diffuse through the "dry" pass before it reaches the region where it may initiate a crack. Since the "wet" pass has a surface open to the atmosphere, the rate of escape of hydrogen is high, and the amount of hydrogen that will reach the highly stressed notched area is much less than for any of the cases studied involving a "wet" pass. The "dry" - "wet" sequence was therefore much less sensitive to cracking than the others involving a "wet" pass.

Postheating Studies

In an attempt to accelerate the escape of hydrogen to the atmosphere, various postheating cycles were imposed on restraint specimens of "T-1" steel welded with Alloy No. 2 electrode. Figure 12 presents the heating and cooling cycles used for each specimen in this study. In Figure 12-I, 15 inches per minute travel speed was employed on a specimen at 7 inches of restraint. To compare these data with data for a larger bead size, another series of tests, presented in Figure 12-II, was made using a travel speed of 6 inches per minute at 8 inches of restraint. Since the heat input was much greater for the specimens welded at the lower travel speed, it was necessary to use a fan to cool specimens from the postheating temperature to room temperature. Without the fan, the specimen would cool so slowly through the temperature range from 200° yo 80°F that the effective time at the elevated temperature would be very difficult to evaluate.

A comparison of curves (A) and (B) reveals that the time required to initiate a crack is decreased by postheating at 125°F. A similar effect is shown by curves (J) and (K) where the maximum postheating temperature is kept constant but the cooling cycle is varied. Curve (K) remains below 150°F, but above room temperature where diffusion is accelerated, causing the cracking time to diminish. However, the time to crack is lengthened as the maximum temperature is increased, going from curve (D) to (E) to (F). It appears that postheating at a very moderate temperature will accelerate cracking, but as the temperature is gradually increased the time to crack is lengthened.

A moderate temperature increase will increase the rate of diffusion, and cause cracking to occur more quickly. Slightly higher temperatures and longer times at temperature, however, appear to effect the escape of hydrogen and reduce the concentration of hydrogen at the fusion line, where cracking of "T-1" steel occurs when welded with Alloy No. 2 electrode. This results in longer time being required to build up a critical concentration of hydrogen. The specimens represented by curves (F) and (G) represent slightly higher temperatures and longer times at temperature. Both of these did not crack.

Specimens represented by curves (H) and (I) were heated at a faster rate. Specimen (H) reached 190°F within 35 minutes from the time of welding. This is almost identical to the maximum temperature of specimen (F) which failed to crack. Apparently specimen (H) cracked because it was not held long enough at the elevated temperature and it did not outgas as much as specimen (F). Specimen (I) reached 220°F in 60 minutes. This was sufficient to reduce the concentration of hydrogen near the region of crack initiation and no crack formed. Specimen (L) was heated very rapidly, reaching 230°F in only 20 minutes from the time of welding, and no crack formed. The extremely fast heating rate used for specimen (M) prohibited cracking by heating to 310°F in 15 minutes from the time of welding.

Thus, the time required to inhibit cracking is a function of the temperature of postheating, and only moderate temperatures are required to inhibit cracking in a single pass bead deposited with a heat input of 32 kji.

The specimens welded at 6 inches per minute were evaluated in a similar manner, except that the heating and cooling cycles were chosen in such a manner that the time at temperature could be evaluated more closely. That is, the specimens were brought to the temperature of interest more rapidly, and after holding for a predetermined time, cooling to room temperature was accelerated.

A similar cracking response was found. The series at 210°F exhibited similar times to cracking as those from (A) through (F). Specimen (O) cracked in 8.5 hours with no postheating. Specimens (P) through (U) were held for increasing times at 210°F immediately after welding. The time to crack was decreased thereafter until cycle (T) which represented nearly 100 minutes at 200°F. Specimen (T) cracked in 16.0 hours. Specimen (U) was held 200 minutes above 200°F, and cracking was avoided by this cycle.

As the temperature of postheating was raised to 310°F cracking was inhibited after only 30 minutes. This is exemplified by curves (V) and (W). An even shorter time at 400°F prevented cracking with cycle (X). To prevent cracking in specimens with the larger bead it is required that higher temperatures or longer times at temperature be used. Apparently, the larger bead presents a longer diffusion path for the escape of hydrogen to the atmosphere. The bead deposited at 15 inches per minute measures 1 cm from the root of the notch to the surface of the bead where hydrogen escapes to the atmosphere. The bead deposited at 6 inches per minute measures about 1.5 cm for the escape path. Thus, it is reasonable to expect the larger bead to be more

sluggish in response to postheating.

If it is assumed that the diffusion rate follows the relationship

$$D = D_o e^{-Q/RT},$$

then the time to crack is proportional to exp. (-Q/RT). It follows that

$$\ln(t_a/t_b) = \frac{Q}{R}(1/T_a - 1/T_b),$$

where t_a is the time required for cracking at postheating temperature T_a, and t_b is the time required for cracking at temperature of postheat T_b. This relationship can be evaluated to solve for Q, the activation energy. Figure 12-II, where cracking was inhibited at two different postheating temperatures, provides the necessary data.

let $T_a = 210^oF$, and $t_a = 180$ minutes.

let $T_b = 310^oF$, and $t_b = 30$ minutes.

then

$$\ln(180/30) = \frac{-Q}{R}(1/372^oK - 1/427.5^oK),$$

and $Q = -10,200$ cal/gm

An independent method of calculting the activation energy was also evaluated. This method uses the time required to <u>initiate</u> a crack at different temperatures. This method can be applied at temperatures for which the escaped hydrogen is small. Figure 13 is an Arrhenius plot of the delay in time required to initiate a crack and the reciprocal of the temperature of postheating. Using data for 0^oF, 80^oF and 125 to 150^oF for six different test conditions, the activation energy for the diffusion of hydrogen under these six conditions

was evaluated.

Values for the activation energy determined by this method ranged from 5.9 to 2.7 kcal. These determinations suffer from the fact that data taken at higher temperatures represent specimens of lower hydrogen content than the low temperature specimens. This supposition is supported by the following argument.

Alloy No. 2 weld metal on A-212 steel at 8 inches of restraint exhibited cracking in a shorter time at room temperature than any other condition examined. The point at 125°F used for this determination falls below the best straight line given by the data, and cracking was indeed accelerated by the increased diffusion rate of hydrogen at the higher temperature. However, the "T-1" (7") and the HY-80 (6") represent less severe or less crack sensitive conditions. They cracked at longer times than the Alloy No. 2 weld metal at both room temperature and 0°F. Consequently, they would be expected to crack at a longer time than the Alloy weld metal at the elevated temperature. The longer time at elevated temperature, however, appears to have allowed for the escape of hydrogen, since both of the elevated temperature points represent cracking times that are <u>much</u> longer than that predicted by the 80 and 0°F data. This relationship should be linear, if the same amount of hydrogen were lost by specimens at each of the three temperatures.

The activation energy values generally decrease as the time required for cracking (at any temperature)increases. This indicates that hydrogen escape at the higher temperatures is playing a more important

role at the time to crack is increased. In an attempt to minimize the scatter due to the higher temperature data, the activation energy values were recalculated using only data from 80 to 0°F. Since the data taken at the 0°F postheating temperature did not represent a specimen held at 0°F immediately after welding, a correction must be made that will make the two treatments comparable. The room temperature specimens were cooled continuously in air from the time of welding. The 0°F specimens were cooled in air for 12 to 15 minutes, until the weld bead and the base metal were at the same temperature. Then the specimen was quenched in an alcohol bath maintained at 0°F. As a first approximation, it was calculated that 18 subtracted from the cracking times of all specimens would yield data for tests at 0°F which could be compared directly with data taken at 80°F. This correction gives all cracking data a common base point in time, and compensates for the fact that the "0°F" tests and the "80°F" tests were held at temperatures above the nominal temperatures.

These data were then replotted as Figure 14 in an attempt to refine the calculated value of activation energy. The calculated activation energy values derived from these data ranged from 8.0 to 2.9 kcal. The lower values were again obtained for the less susceptible conditions found at longer cracking times. The effect of escape of hydrogen is apparent.

The activation energy seems also to be a function of the composition of the steel through which diffusion occurs. The Alloy No.2 weld metal has a higher activation energy than the two base plates,

"T-1" and HY-80.

Thus, postheating at temperatures typical of preheating practice was effective in eliminating delayed cracking in alloy steels. The time at temperature required depends on the size of the weld and can be reduced markedly by raising the temperature moderately. The basic equation for diffusion in infinitely long cylinders is of the form

$$f = Dt/r^2,$$

where f is a time function related to the residual hydrogen fraction U, and

$$U = \frac{\text{residual hydrogen}}{\text{initial hydrogen}}$$

Assuming that there is a value of f, below which cracking will not occur in specimens welded with the water atmosphere, then the fraction D/r^2 is a constant. Since the relationship between D and absolute temperature (T) is known to be of the form

$$D = D_o e^{-Q/RT},$$

a curve can be calculated to relate the postheating temperature to the bead diameter. Such a curve is presented as Figure 15 where bead diameter is plotted against the temperature at which cracking can be eliminated by 1 hour of postheating. The base point of 212°F was assumed to inhibit cracking in the 1 cm bead. This is a conservative estimate taken from the data presented for postheating of "T-1" steel welded at 15 in. per minute in argon with 1% H_2O added. The best estimate of

the activation energy was chosen as -7500 cal for the calculation of the postheating temperatures required for various bead diameters.

The calculated curve predicts a 1 hour postheating temperature of 270°F for a bead diameter of 1.5 cm (0.6 inches) corresponding to welds deposited at 6 inches per minute. The postheating data presented in Figure 12-II for this condition are in excellent agreement with this predicted temperature. The calculated curve reveals that cracking can be prevented in a 2 inch bead by postheating for 1 hour at 520°F.

Spray vs. Drop Transfer

Cracking tendency was studied as a function of the mode of metal transfer in a welding atmosphere of argon with 1% H_2O. The results are listed in Table 9. Using the same amperage and heat input with both straight and reversed polarities, welds were made on HY-80 plates with Alloy No. 2 electrode and A-212 plates with the triple deoxidized electrode. The straight polarity was used to obtain the drop transfer of the metal. No difference was found in the critical restraint for tests made at the same amperage with straight and reversed polarities for the HY-80 and a difference of only 1/2 inches of restraint was found for the A-212 steel. However, the time required to produce cracks at a level just above the critical restraint is much shorter for both steels when welded with straight polarity. In the HY-80 series of tests, the mode of metal transfer was also changed from spray to drop transfer by decreasing the amperage from 250 to 190 amperes for reverse polarity welds. Heat input was kept constant for these welds by changing the travel speed. At the lower amperage, the cracking tendency was decreased, the critical restraint increasing from 7 to 8 inches. In summary, the mode of metal transfer appears to exert only a minor influence on the cracking tendencies of the steels tested.

Effect of Prior Microstructure in HY-80 Steel

The crack susceptibility of low-chemistry HY-80 as affected by prior microstructure was determined. Table 10 presents data for both Steel No. 2 and No. 5. Photomicrographs of the prior base plate structures are presented in Figure 2, which also summarizes the test results. Variation of the microstructures was obtained by austenitizing at 1650°F and then either annealing, normalizing, spray-quenching, spray quenching and tempering, or spheroidizing the steel. It is evident from the microstructures and the crack sensitivities that cracking sensitivity increases progressively as the carbide size or non-homogeneity of the steel increases.

Relatively massive ferrite and bainite regions produced by annealing are the most unfavorable of the microstructures shown. Apparently, the non-homogeneities presist in the heat affected zone after welding. The resultant high carbon areas play a dual role favoring heat-affected-zone hydrogen embrittlement. First, they favor the retention of austenite to low temperatures. The austenite releases hydrogen during the cooling cycle due to decreasing solubility. Transformation of austenite at low temperatures further increases the amount of excess hydrogen in the lattice. The second role of the high carbon areas is to provide hard brittle spots and a wide variation of hardness in the heat affected zone.

Table 11 is offered in support of the postulated effects of the non-homogeneities on the hardness of the heat affected zone. Diamond pyramid hardness taken with a 1 Kg load are presented for the heat

affected zone of specimens whose prior structures include annealed, spheroidized, normalized, and spray-quenched conditions. Although the average equivalent Rockwell "C" hardness for the various structures is 43.0 to 44.0, the range of hardness (in Rockwell "C" equivalents) for the annealed specimen represents a spread of 9 points from 38 to 47 "C". The range found for the spheroidized and the normalized structures is only 3 points, and the spray quenched specimen was most uniform with a spread of only 2 points in Rockwell "C" equivalent hardness.

Weld metal hardness for these specimens, also presented in Table 11, was lower in every case than the HAZ hardness. Cracks were examined metallographically, and cracks were found to have initiated in the harder HAZ structures of HY-80.

Increased susceptibility to cracking was found for 1-inch-low-chemistry HY-80 plate as the prior structure was varied in the order spray-quenched, normalized, spray-quenched and tempered, spheroidized, and annealed. The critical restraint above which cracking would be initiated was 8 inches for the spray-quenched plate, and 6 inches for the annealed plate. For the 1-1/2 inch high chemistry heat, tested in both the spray-quenched and tempered, and the normalized conditions, the normalized structure was found to be about as sensitive to cracking as the spray-quenched and tempered structure. Cracking was initiated, however, at a lower level for the 1-1/2 inch high chemistry plate for both heat treatments when compared with the 1 inch low chemistry plate.

These results clearly contradict the findings of several investigators[38,39,40,41] who report that steels with large carbides, which do not go into solution readily during rapid thermal cycles, behave as lower carbon steels when welded, and appear definitely less sensitive than fine-carbide steels. However, Koziarsky[42] gives complete data of a Cr-Mo steel having very fine carbides and yet seeming not sensitive at all. Also, Sims and Banta[39] report abnormally high cracking in C-Mn steels. They found that manganese banding, resulting from segregation that occurs during the ingot freezing and persists through processing, caused the abnormal cracking.

Effect of Plate and Electrode Composition

Composition of HY-80

In addition to the low chemistry heat of 1 inch HY-80, and the 1-1/2 inch plate of high chemistry HY-80 previously discussed, three heats of high chemistry HY-80 were studied at 1 inch plate thickness. One heat contained a special addition of 0.003% rare earths. Another was given no special treatment, and the third was vacuum melted with limits of 0.010% placed on the P and S. Results of the cracking tests are presented as Table 12.

The tests showed the greater sensitivity of the high chemistry heats, and of the greater plate thickness. The vacuum melted heat showed considerable improvement in resistance to cracking over the conventional heat. Its resistance was slightly less, however, than that found for the low chemistry heat. The addition of rare earths did not appear to reduce the cracking tendency.

Rare earth additions to some ferrous alloys reportedly[43] reduces their sulfur, nitrogen and hydrogen content and enhances physical properties such as impact, transition temperature, ductility, etc. They also act as grain-refining agents and prevent grain coarsening and hot tearing. Besides the chemical affinity to sulfur, oxygen and nitrogen, the rare earths dissolve very high amounts of hydrogen. At 2000°F the solubility of hydrogen in lanthanum is 2000 times greater than in iron. At lower temperatures this effect is even more pronounced, Lanthanum dissolves over 65,000 times as much hydrogen at 750°F when compared with iron.

Koziarski[42] suggests that the use of rare earths should be analyzed in welding applications with the intention of reducing cracking sensitivity in ferrous and aluminum alloys. In view of these observations the special heat was expected to be improved in crack resistance by rare earth additions. However, no benefits were observed in this study of hydrogen embrittlement in steel weldments.

In addition to the various heats of HY-80 steel, 5 steels offering a range of hardenabilities were investigated to determine the influence of plate composition on delayed cracking. Table 13 summarizes the results of this investigation for welds deposited with Alloy No. 2 electrode. Generally, the crack susceptibility increased in the heat affected zone, as the carbon equivalent of the base plate, increased. A more detailed analysis of these test results will be made after the discussion of the effect of the electrode composition and the locus of crack initiation.

Electrode Composition

The effect of the electrode composition on the crack sensitivity is presented as Table 14 for "T-1" and A-302 steel plates. Three alloy electrodes were tested on "T-1" steel plates. Their characteristics were quite similar. The triple deoxidized electrode used on "T-1" steel caused cracking to initiate at lower restraint than any of the alloy electrodes. The carbon equivalent of this electrode was very low, but the hydrogen content was over 2 ppm and the electrode was copper coated to prevent oxidation. Kudva[44]

found that this copper coating inhibited the excape of hydrogen from the electrode during baking prior to welding. This resulted in the introduction of additional amounts of hydrogen into the weldment and therefore cracking occurred at lower restraint. This electrode also caused cracking to occur in A-302 at lower restraint than did the alloy electrode.

The A-302 steel exhibited HAZ cracking at the same restraint level, whether welded with a commercial alloy electrode or with the special pure iron electrode. However, deposition of a 25-20 austenitic stainless steel was effective in preventing HAZ cracking of sensitive A-302 steel. At the highest restraint, hot cracks appeared in the stainless weld metal. Clearly, the only reasonable explaination of the behavior at the lower restraints is that the solubility of hydrogen in the austenitic bead is so high that hydrogen is drawn from the heat affected zone into the weld metal. This conclusion is supported by the test results for the dry argon atmosphere on A-302 welded with the triple deoxidized and the alloy electrodes. With both electrodes the critical restraint is the same for both the dry atmosphere and the atmosphere containing 1% H_2O. Cracking time was greatly extended for tests made in the dry atmosphere, because the hydrogen content was so slight as to require a long time for a critical concentration to accumulate at the triaxiality region. Cracking was shown by the transducer signal to be a discontinuous process in these tests. Similarly, all tests that exhibited long time cracking exhibited the discontinuous cracking

response described by Troiano[6].

Pure iron welds inhibited cracking in "T-1" steel and in 1-1/2 inch HY-80 steel up to the highest restraint level. The results suggest that low strength weld metal may be beneficial to cracking resistance, provided the base metal HAZ is not excessively susceptible to cracking, as in the case of A-302 steel.

Locus of Crack Initiation

Metallographic sections were taken from restraint specimens to determine the locus of cracking at the root of the bead near the notch where cracks initiate. Results of this survey are presented as Table 15. The position of cracking was located as weld metal, fusion line or heat-affected zone. The fusion line was indicated when the crack followed the interface between the weld metal and the heat-affected zone so closely that it was uncertain which material contained the crack. In general, when hardenable weld metal was deposited on low-hardenable plate, the source of cracking was in the weld metal. As the hardenability of the plate increased, the crack moved to the heat-affected zone. This effect is shown in Figure 16 for HY-80 and A-212 base metal welded with Alloy No. 2 weld metal.

Restraint level during welding can also shift the locus of cracking. Figure 17 shows that identical welding conditions produce base-metal cracking in HY-80 steel when welded with a 5-inch bead but weld metal cracking when welded with a more highly restrained 3-inch bead. In the latter case, cracking is so early that it lies outside the definition of delayed cracking. It is probable

that the cracking is due to inability of the weld metal to adjust by plastic flow to the confinement of the joint rather than to the hydrogen-martensite interaction characteristic of delayed cracking.

Several specimens were prepared at the critical restraint level and examined at high magnification for microcracks. Microcracks were found in all specimens examined at the critical restraint. Their location was in every case in the more hardenable structure. Subsequently, specimens which had been welded at restraint levels below the critical restraint were examined to determine if microcracks were present. Their presence in these specimens would indicate that the effect of stress is only to expand existing cracks, but not to cause their initiation in the presence of hydrogen. Examination of specimens PR27, HAP3, ER13, M1, A-201-3 and A-201-1 revealed no microcracks. Thus, it is concluded that Troiano's[6] conclusion is correct in that hydrogen is non-damaging if the level of restraint is insufficient to induce the critical hydrogen concentration.

Microcracks observed for A-212 welded with the more hardenable Alloy No. 2 electrode, and "T-1" welded with the less hardenable triple deoxidized electrode were photographed and presented as Figure 18. Note that the crack initiates not at the notch but in the region of maximum triaxial stress near the notch. This is depicted in the two photomicrographs of the same crack in "T-1" steel at 100X and 65X. This crack is discontinuous. The effect is not apparent in the photomicrographs of the micro-crack in specimen BR22 of A-212 steel. This specimen is presented at 500X in both the etched and unetched conditions to clarify the path taken by the crack.

Hardness Survey of Weld and HAZ

A survey of the hardness of the weld metal and the coarse grained HAZ areas was made for welds deposited with Alloy No. 2 electrode and six base metal compositions of varying hardenability. Two weld deposits of the lower hardenability triple deoxidized electrode were surveyed. The Vickers diamond pyramid hardness was used on the coarse grained area. A load of 1 Kg was used so that hardness of individual grains could be determined in the heat affected zone. The weld metal survey was made with the Rockwell 30N hardness, since fewer determinations with this test would yield the desired results and the hardness of individual grains was not sought. These data are presented as Tables 16 and 17.

Base metal structures were as-rolled, normalized, and quenched and tempered. Excessive variation in hardness of the grains in the HAZ was not noted except for the normalized and as-rolled structures of HY-65 and A-212 steels, respectively. Hardness of the weld metal structures were quite uniform for all beads examined.

When the hardness averages of the weld metal and HAZ areas examined were compared with the locus of crack initiation, it was found that in every case cracks initiated in the harder structure in the weldment.

Hardenability of Base Plate

An attempt was made to evaluate more critically the relationship between carbon equivalent and cracking response of the various base metals tested. For this evaluation a direct comparison of cracking

response was made with the carbon equivalent for test conditions exhibiting heat affected zone cracks only, as the carbon equivalent of the weld metal could only be estimated because of dilution effects.

The Winterton[25] formula for alloy steels was evaluated for each of the steels exhibiting heat-affected-zone cracking when welded with Alloy No. 2 electrode. The critical restraint was estimated to the nearest 1/2 inch, and the restraint required to produce a crack at 2 hours from the time of welding was also estimated to the nearest 1/2 inch. These data were plotted using carbon equivalent as the independent variable and presented as Figure 19. The relationship is not apparent from this plot, but an analysis of the data revealed that the factor of 6 for Mn in Winterton's formula was the cause of much of the scatter of the data. Therefore, the carbon equivalent was calculated using the Winterton formula except that the Mn factor was changed. Values of 3, 4, 5, and 6 were used in the calculations. Each of the new sets of carbon equivalents were then plotted on separate graphs as functions of the restraint for both the critical level and the 2 hour crack level. The deviation from linearity was calculated for each of the data points using the carbon equivalent as the dependent variable. Then the average percent deviation of all data on each curve was calculated. These data are compared in Figure 20 in terms of the percent deviation obtained for each of the formulae of various Mn factors. The function is readily seen to have a minimum between 3 and 5. To evaluate the minimum in this function

Newton's forward interpolation formula was employed. The polynomial function derived from Newton's formula was minimized and evaluated at the minimum. This was done for both the values corrected for 2 hour cracks, and the critical restraint (corrected estimates of the maximum no crack restraint). The results, shown in Figure 20, clearly indicate that the Winterton formula is best fitted to the cracking data with a factor of Mn/4.0 instead of Mn/6. When Mn/4 is used the deviation from linearity is only 1% for the critical restraint curve and 1.3% for the values corrected to 2 hour cracking. These relationships, also presented in Figure 19, clearly depict that crack susceptibility increases with the carbon equivalent calculated from the Winterton formula using Mn/4.

In view of these results the Battelle formula[23] which employs the Mn/4 and Si/4 was fitted to the cracking data and presented as Figure 19. This formula differs from the corrected Winterton formula in that the Winterton formula does not evaluate the effect of silicon. The Battelle formula did not improve the fit found for the corrected Winterton formula, since the variation in silicon content was not large for the steels under consideration. It is concluded that the carbon equivalent formula is useful for predicting crack susceptibility, and that Mn/4 yields more consistent results than Mn/6.

Non-Martensitic Heat Affected Zones

Attempts were made to observe the delayed-cracking sensitivity in welded specimens in which the composition and cooling rates do not give rise to the formation of martensite. The difficulty in this

problem is that martensite readily forms in all but the very low hardenability steels even at moderate cooling rates. In tests on A-212 steel welded at 250 amperes and 6 inches per minute travel, appreciable martensite was produced in the HAZ, and delayed cracking was observed.

Further tests on A-201 steel resulted in weld zone structures apparently free of martensite. Both metallographic and hardness survey techniques were employed in an effort to detect the presence of martensite. Results of the cracking tests are presented as Table 18. Cracking could not be initiated in specimens welded under even the most severe conditions with either the triple deoxidized electrode or the alloy electrode. A survey of the microhardness revealed that the weld metal and the HAZ hardness was less than DPH of 300. These data are presented in Table 19. No evidence of the presence of martensite could be found and these specimens did not crack even under the most severe conditions tested. Further, metallographic examination of the most severe condition tested for A-201 revealed no microcracking.

Cracking Tests on Maraging Steel

One-inch plate of 18% Ni maraging steel was tested in both the solution treated and the maraged conditions. A special maraging electrode was used for these tests. The maraging steel was also tested in the annealed condition using Alloy No. 2 electrode. The data are given in Table 20. Despite the application of the maximum restraint obtainable in the specimen, no cracking occurred in weldments

deposited in an atmosphere of 5% H_2 + 1% H_2O. The resistance to cracking of the "carbon-free" martensite of the maraging steel suggests that carbon segregation contributes to cracking by producing regions of high carbon martensite which is brittle and susceptible to cracking in the presence of hydrogen. This concept is supported by previous tests on HY-80 steel in which annealed plates containing coarse carbides were found to be more crack sensitive than quenched plates in which the carbon was uniformly distributed.

Retainte Austenite Measurements

It has been suggested that delayed cracking may be caused, at least in part, by austenite retained to room temperature which transforms isothermally at a relatively slow rate over a period not exceeding two hours. An attempt was made to evaluate this effect. Retained austenite determinations made within one hour after welding were repeated after successive time intervals up to 2 days from the time of welding. The amount of retained austenite in the HAZ and the weld metal was found to be small. No variation in the amount of retained austenite was found with time from welding. Data taken in these determinations are presented in Table 21. Thus, no evidence was found to support isothermal decomposition of austenite as a contribution mechanism to delayed cracking. However, it must be noted that these determinations were not capable of evaluating the possible transformations occurring from the time of welding to one hour after welding.

SUMMARY

SUMMARY

The findings of this investigation can be summarized as follows:

1. Delayed cracking could not be initiated in weldments made in a dry argon atmosphere except in a Mn-Mo steel which was particularly susceptible to delayed cracking.

2. The susceptibility to delayed cracking was found to be proportional to the hydrogen content of the welding atmosphere. The amount of hydrogen in the welding atmosphere in free (H_2) or combined (H_2O) form appeared to act in a cumulative manner in the range from 0 to 6% hydrogen.

3. The time required to form a crack was related by inverse functions to the hydrogen content of the welding atmosphere and the restraint level of the Lehigh restraint specimen.

4. The cracking response of low chemistry HY-80 welded with cellulosic electrodes compared almost exactly with gas metal-arc weldments made in an atmosphere of argon with 5% H_2 + 1% H_2O added. Response to delayed cracking of this steel welded with E-7016 and E-9015 electrode was comparable with gas metal-arc weldments made in an argon atmosphere with 1% H_2O.

5. The mode of metal transfer appears to exert only a minor influence on the cracking tendencies of the steels tested.

6. Studies of the effect of prior heat treatment on the crack sensitivity of HY-80 steel revealed that resistance to delayed cracking is enhanced by a finer carbide dispersion.

7. Five heats of HY-80 steel were investigated. The crack resistance of HY-80 steel was enhanced by vacuum melting, but the addition of .003% rare earths did not increase the resistance to cracking. Greater sensitivity to cracking was exhibited by the high chemistry steel and by the heat of greater plate thickness.

8. The critical restraint is that level of restraint beyond which cracking will be initiated. The critical restraint for heat affected zone cracking was found to be inversely proportional to the carbon equivalent of the base metal. The data indicated that a better evaluation of the crack susceptibility of the HAZ is given by the Battelle factors for Mn and Si than by the Winterton formula, because manganese and silicon play more important roles than the Winterton formula would predict.

9. Specimens of "t-1" and ASTM A-302 steels were welded with pure iron, low carbon steel, triple deoxidized and low alloy electrodes. The electrode composition exerted only a minor influence on the susceptibility of the plate to HAZ cracking, except that welds deposited with pure iron on "T-1" steel and HY-80 steel did not produce cracks up to the maximum restraint. Welds deposited with 25-20 Cr-Ni austenitic stainless steel eliminated delayed cracking on the crack sensitive A-302 steel, presumably by acting as a reservoir for the dissolved hydrogen. At higher restraints, however, hot cracks developed in the stainless steel welds.

10. One inch plates of 18% nickel maraging steel were welded under argon containing 1% H_2O + 5% H_2 with a special 18% nickel

maraging electrode and also with a low alloy electrode. No cracking occurred even at the highest restraint obtainable in the specimen. The resistance to cracking of carbon free martensite in maraging steel and the increase in crack susceptibility of HY-80 with coarser carbide dispersion suggest that carbon segregation contributes to cracking by producing regions of brittle high carbon martensite which favors cracking in the presence of hydrogen.

11. Studies on A-201 and A-212 steels indicated that delayed cracks could not be produced in the absence of martensite.

12. Metallographic samples were taken from the center of cracked restraint tests to determine the locus of crack initiation. In general, when hardenable weld metal was deposited on low hardenability plate, the source of cracking was in the weld.metal. As the hardenability of the plate increased, the cracks were transferred to the heat affected zone.

13. Postheating at temperatures typical of preheating practice were effective in eliminating delayed cracking in alloy steels. The time at temperature required depended on the size of the weld and could be reduced markedly by raising the temperature moderately.

Bibliography

1. Zapffe, C. A.,
"Iron-Hydrogen",
Metals Handbook (1948), ASM, 1208-1209.

2. Sieverts, A.,
"Die Aufnahme von Gasen durch Metalle"
Zeit.Metallk. (1929), 21, (2), 37-44

3. Darken, L. S.
"Diffusion of Carbon in Austenite with a Discontinuity in Composition",
Trans AIME (1949), 180, 430-438.

4. Hobson, J. D.,
"The Diffusion of Hydrogen in Steel at Temperatures -78° to 200°C",
J. Iron and Steel Inst. (1958), 189, 315-321.

5. Sykes, C., Burton, H. H., Gegg, C. C.,
"Hydrogen in Steel Manufacture",
Ibid (1947), 156, 173-174.

6. Troiano, A. R.,
"The Role of Hydrogen and Other Interstitials in the Mechanical Behavior of Metals",
Trans ASM (1960), 52, 54-80.

7. Troiano, A. R.,
"Embrittlement by Hydrogen and Other Interstitials",
Metal Progress (1960), 77, 112-117.

8. deKazinski, F.,
"A Theory of Hydrogen Embrittlement",
J. Iron and Steel Inst. (1954), 177, 85-92.

9. Zapffe, C., Discussion to
"Practical Importance of Hydrogen in Metal-Arc Welding of Steel",
Trans ASM (1947), 39, 190-191.

10. Zapffe, C. A., Sims, C. E.,
"Hydrogen Embrittlement and Defects in Steel",
Trans AIME (1941), 145, 225-261.

11. Sims, C. E.,
"Behavior of Gasses in Solid Iron and Steel"
Gasses in Metals (1953), ASM.

12. Bastien, P., Azou, P.,
"Effect of Hydrogen on Deformation and Fracture of Iron and Steel in Simple Tension",
Proc. 1st World Metall. Congr., (1951), ASM 535-552.

13. deKazincazy, F.,
"A Theory of Hydrogen Embrittlement",
J. Iron and Steel Inst. (1954), 177, 85-92.

14. Petch, N. J., Stables, P.,
"Delayed Fracture of Metals Under Static Load",
Nature (1952), 169, 842-843.

15. Johnson, J. G., Morlet, J. G., Troiano, A. R.,
"Hydrogen, Crack Initiation and Delayed Failure in Steel",
Trans. AIME (1958), 212, 528-535.

16. Morlet, J. G., Johnson, H. H., Troiano, A. R.,
"A New Concept of Hydrogen Embrittlement in Steel",
J. Iron and Steel Inst., (1958), 188, 37-44.

17. Steigerwald, E. A., Schaller, F. W., Troiano, A. R.,
"Role of Stress in Hydrogen Embrittlement",
Trans AIME (1960), 218, 832-841.

18. Steinberger, A. W., Stoop, J.,
"Studies of the Crack Sensitivity of Aircraft Steels",
Welding J. (1952), 31, 527s-542s.

19. Bibliographical and Practical Experience Report on Cold Cracking in the Heat Affected Zone,
Commission No. 9, "Weldability", IIW, IX-110-54.

20. Berry, J. T., Allan, R. C.,
"A Study of Cracking in Low-Alloy Steel Welded Joints",
Welding J. (1960), 39, 105s-116s.

21. Bell, Patricia, E.,
Bibliography on The Effects of Hydrogen Embrittlement on Metals: 1952 to Present,
Los Alamos Scientific Laboratory of the U. of Calif.,
Los Alamos, New Mexico., (Dec. 1958), 19pp., available from Office of Technical Services, U. S. Department of Commerce, Washington 25, D. C.

22. Dearden, J., O'Neill, H.,
"A Guide to the Selection and Welding of Low Alloy Structural Steels",
Trans Inst. Weld., U.K. (1940), 3, 203-214.

23. Voldrich, C. B., Martin, D. C., Harder, O. E.,
"Notch-bead Slow-bend Tests of Carbon-Manganese Steels",
Welding J. (1947), 26, 489s-507s.

24. Stout, R. D., Doty, W. D.,
"Weldability of Steels", Welding Research Council, (1953),
New York, 381 pp.

25. Winterton, K.,
"Weldability Prediction from Steel Composition to Avoid Heat-Affected Zone Cracking",
Welding J. (1961), 40, 253s-258s.

26. Heuschkel, J.,
"Steel Properties Related to Welded Performance",
Ibid. (1949), 28, 135s-152s.

27. Stout, R. D., Tor, S. S., McGeady, L. J., Doan, G. E.,
"Quantitative Measurement of the Cracking Tendency in Welds",
Welding J. (1946), 25, 522s-531s.

28. Stout, R. D., Tor, S. S., McGeady, L. J., Doan, G. E.,
"Some Additional Tests on the Lehigh Restraint Specimen",
Ibid (1947), 26, 373s-396s.

29. Agnew, S. A.,
Root Bead Welding of Structural Steel Restraint Specimens at Low Atmospheric Temperatures,
Canada Dept. of Mines and Technical Surveys,
Research Report No. PM222, (Sept. 27, 1957), Ottawa.

30. Beachum, E. P.,
An Investigation into the Causes of Delayed Cracking in Steel Weldments,
Ph.D Dissertation, Lehigh University, 1960.

31. Beachum, E. P., Johnson, H. H., Stout, R. D.,
"Hydrogen and Delayed Cracking in Steel Weldments",
Welding J. (1961), 40, 155s-159s.

32. Blake, P. D.,
"Measurements of the Diffusible Residual, and Total Hydrogen Contents of Weld Metal",
Brit Welding J. (Mar. 1958), 12-15.

33. Derge, G., Peifer, W., Richards, J. H.,
"Sampling and Analysis of Steels for Hydrogen",
Trans AIME (1948), 176, 219-247.

34. Derge, G., Duncan, E. E.,
"Thermal Segregation: A Mechanism for the Segregation of Hydrogen",
Ibid (1950), 188, 884-885.

35. Averbach, B. L., Cohen, M.,
"X-Ray Determination of Retained Austenite by Integrated Intensities",
Ibid (1948), 176, 401.

36. Cullity, B. D.,
Elements of X-Ray Diffraction,
Addison-Wesley (1956).

37. Bierwirth, G.,
"Die rontgenographische Bestimmung des Restaustenits in einsatzgeharteten Stahlen",
Sonderdruck aus Materialprufung, Wernerwerk fur Messtechnik. (1961), 6, Siemens & Halske Aktiegesellschaft.

38. Hoyt, S. L., Sims, C. E., Banta, H. M.,
"Metallurgical Factors of Underbead Cracking",
Welding J. (1945), 24, (9), 433s-445s.

39. Sims, C. E., Banta, H. M.,
"Development of Weldable High-Strength Steels",
Ibid (1949), 28, (7), 326s-336s.

40. Folkhard, E.,
"Die Riss-und Sprodbruchanfalligkeit hochfester Baustahle",
Schw u Schn (1952), 4, (5), 139-154.

41. Schaoffler, A. L., Campbell, H. C., Thielsch, H.,
"Hydrogen in Mild Steel Weld Metal",
Welding J. (1952), 31, (6), 283s-309s.

42. Koziarsky, J., Discussion to
"Studies of the Crack Sensitivity of Aircraft Steels"
Ibid (1951), 30, (2), 163-166.

43. Knapp, W. E., Bolkcom, W. T.,
"Rare Earths Improve Properties of Many Ferrous Metals",
Iron Age (1952), 170, Part I, 129-134; Part II, 140-143.

44. Knapp, W. E., Bolkcom, W. T.,
Effect of Cathodic Charging on the Crack Sensitivity of Steel Weldments,
M. S. Thesis (1963), Lehigh University.

45. Fromberg, R. P., Barnett, W. J., Troiano, A. R.,
"Delayed Failure and Hydrogen Embrittlement in Steel",
Trans. ASM (1952), 47, 892-925

Table 1

Chemical Composition of Steel Plates

(% Element by Wt.)

Steel No.	Steel Description	Code	C	Mn	Si	P	S	Ni	Cr	Mo	Co	V	Cu	Al	Ti	Zr	B	N	H(ppm)	O
1	Navy HY-80	Y	.18	.21	.23	.01	.014	2.93	1.82	.40	---	---	---	---	---	---	.03	.009	0.2	.0014
2	Navy HY-80 (low chem)	H	.18	.36	.17	.018	.016	2.25	1.22	.30	---	---	---	---	---	---	---	.016	.8	.0014
3	Navy HY-80*	HR	.16	.35	.28	.03	.009	2.8	1.7	.46	---	<.01	.07	.075	---	---	---	.015	1.0	.0015
4	Navy HY-80**	HAP	.18	.36	.26	.01	.003 .008	2.91	1.59	.51	---	---	---	---	---	---	---	.003	.6	.0014
5	Navy HY-80 (1-1/2")	HH	.15	.26	.18	.01	.022	2.84	1.52	.45	---	---	---	---	---	---	---	.007	1.2	.0006
6	Navy HY-65	G	.12	.48	.20	.013	.032	2.16	.06	.39	---	.11	.70	.058	---	---	---	---	---	-----
7	"T-1"	PR	.15	.93	.27	.015	.022	.89	.48	.44	---	.06	---	---	---	---	.003	---	---	-----
8	ASTM A201	A201	.11	.69	.23	.017	.025	---	---	---	---	---	---	---	---	---	---	---	---	-----
9	ASTM A203	ER	.15	.64	.24	.01	.026	3.64	.05	.05	---	.02	---	.019	.006	---	---	---	---	-----
10	ASTM A212	BR	.32	.71	.24	.02	.019	.02	.03	.01	---	---	---	.005	---	---	---	---	0.1	-----
11	ASTM A302	A	.24	1.37	.24	---	---	.28	.20	.47	---	---	.018	---	---	---	---	---	---	-----
12	18% Nickel Maraging	M	.03	.06	.01	.004	.009	18.51	.05	5.00	8.09	---	---	.11	.34	.01	.004	---	.3	-----

* 0.003 wt % rare earths added

** Vacuum melted, vacuum poured as 470 pound ingot, forged between 2200°F and 1800°F

Table 2 - Heat Treating Data

Steel No.	Specimen Identification Code	Conditions Tested	Heat Treating Temperatures (°F) and Times (hrs.)
1	Y	Normalized	Austenitize 1650°F, 1-1/2 hrs.
2	H	Annealed, spheroidized, normalized, spray-quenched & tempered, spray quenched	Austenitize 1650°F, 1-1/2 hrs. stress relieve 1250°F, 1-1/2 hrs. spheroidize 1250°F, 36 hrs.
3	HR	Normalized	Austenitize 1650°F, 1-1/2 hrs.
4	HAP	Normalized	Austenitize 1650°F, 1-1/2 hrs.
5	HH	Normalized, spray-quenched & tempered, spray quenched	Austenitize 1650°F, 2-1/4 hrs. stress relieve 1250°F, 2-1/4 hrs.
6	G	Normalized	Austenitize 1750°F, 1 hr.
7	PR	Quenched & tempered	Austenitize 1700°F, 1 hr. stress relieve 1200°F, 1 hr.
8	A201	As rolled	
9	ER	As rolled	
10	BR	As rolled	
11	A	As rolled	
12	M	Annealed maraged	Solution treatment 1500°F, 1 hr. solution treatment 1500°F, 1 hr.; marage 900°F, 3 hrs.

Table 3

Chemical Composition of the Welding Electrodes

(% element by wt)
Electrode diameters: 1/16" except pure iron 3/32"

Element	Triple Deox.*	Al Deox.*	Alloy No. 1*	Alloy No. 2	Alloy No. 3*	Pure Fe	310SS	18% Ni Maraging
C	.05	.12	.034	.05	.030	.003	.09	.03
Mn	1.48	1.27	1.66	1.32	1.90	<.03	1.78	---
P	.015	.016	.003	.009	.002	.001	.014	.005
S	.014	.025	.008	.012	.003	.008	.012	.007
Si	.56	.47	.23	.55	.30	<.03	.47	.06
Ni	.09	.09	1.85	1.32	1.70	.04	21.55	18.31
Cr	.03	.06	.19	.09	.16	.02	27.10	.07
Mo	.02	.04	.24	.43	.31	.01	.06	4.60
Co	----	----	----	----	----	----	.05	7.90
V	----	----	.03	.15	----	<.01	----	----
Al	.06	.052	.019	----	.034	----	----	----
Ti	.10	----	----	----	.06	----	----	.35
Zr	.04	----	----	----	.034	----	----	----
N	.008	.009	----	.011	----	< .01	----	----
H (ppm)	2.1	1.3	----	0.7	----	0.9	----	5.6
O	.0257	.0135	----	.0104	----	.059	----	----
Cu	----	.17	.08	----	.04	< .01	.04	----

* Electrodes covered with protective copper coating

Table 4

Summary Table of Diffusible Hydrogen Determinations

Steel No(s).	Electrode	Welding Conditions	Average Evolution cc's (H_2)/5" Weld
2	E6010, E9010	27v, 180 amps, 8.5"/ min, 34.2 kji	3.1
2	E7016, E9015	22v, 200 amps, 7.7"/ min, 34.2 kji	0.1
1, 2, 10*	Alloy No. 2 & Triple Deox.	32v, 250 amps, 15"/ min, 32.0 kji, atmosphere of 1% H_2O in argon	<0.1
2	Alloy No. 2	36v, 240 amps, 15"/ min, 34.6 kji, atmosphere of argon with 5% H_2 + 1% H_2O	0.3

* Condition of Steel No. 10 was as rolled. Steel No. 2 was tested in normalized condition and annealed condition, while Steel No. 1 was tested only in normalized condition.

Table 5

Comparison of Diffusible, Residual and Total Hydrogen Contents

Low chemistry HY-80 (Steel No. 2) specimen 1" x 3/8" x 5" welded with aluminum deoxidized electrode, DCRP, 250 amperes, 30 volts, 13.5 inches/minute

Specimen No. Wt (gms)	% H_2 in Argon Shield Gas	CC's H_2 per Inch of Weld			Total CC's H_2 From Bead and Base Metal	
				Total	Per 100g Bead Deposited	Per 100g Section of Bead & Base Metal
1 - 273	10	----	----	1.04	18.2	1.9
2 - 274	10	----	----	1.05	18.4	1.9
		Diffusible	Residual	Sum (D+R)		
3 - 267	10	0.05	0.54	0.59	11.0	1.1
4 - 256	10	0.01	0.45	0.46	8.4	.90
5 - 258	0	0.00	0.12	0.12	2.0	.23
6 - 271	0	0.00	0.18	0.18	3.0	.33

SAMPLE CALCULATION

From Fromberg (45), at S.T.P. 1cc H_2/100g Fe = .896 ppm

Therefore,

$$\frac{\text{equivalent cc's evolved}}{\text{inch weld}} = \frac{\text{PPM}}{.896} \times \frac{\text{Total specimen wt. (gms) after welding}}{\text{100 gms x total bead length (ins)}}$$

Residual H_2 determination for sample No. 6

$$\frac{\text{cc's total}}{\text{inch weld}} = \frac{0.3}{89.6} \times \frac{271}{5.0} = 0.18$$

Table 6

Comparison of Cracking Effects of Hydrogen and Water Additions to the Welding Atmosphere

Lehigh restraint test of normalized low chem HY-80 (Steel No. 2) welded with Alloy No. 2 electrode, DCRP, spray transfer

Welding Conditions	Atmosphere	Restraint	Cracking Time
245A, 36V, 15 in/min.	5% H_2 + 1% H_2O in argon	5	no crack
		5-1/2	no crack
		6	0.7 hr.
		7	0.2 hr.
245A, 34V, 15 in/min.	5% H_2 in argon	5	no crack
		6	1.5 hr.
		7	0.6 hr.
		8	0.3 hr.
		8 (3" bead)	0.15 hr.
240A, 34V, 15 in/min.	1% H_2O in argon	5-1/2	no crack
		7	no crack
		8	2.3 hr.
320A, 33V, 19 in/min.	dry argon	8	no crack

Table 7

Coated Electrode and SIGMA Weldments Compared on Low-Chemistry HY-80 (Steel No. 2) in Response to Delayed Cracking

Heat Treatment	Electrode	Inches Restraint	Cracking Time	Remarks
Normalized	6010	4	no crack	
		5	no crack	
		5-1/2	1.0 hr.	
		6	0.3 hr.	
Normalized	9010	5	no crack	
		6	0.3 hr.	
Annealed	9010	5-1/2	no crack	
		6	4-8 hrs.	Slow crack
		6-1/2	0.15 hr.	Not considered delayed by definition
Normalized	7016	6	no crack	
		8	no crack	
		8	2.1-12.1 hr.	Slow crack
		8(3" bead)	7.9-14.3 hr.	Slow crack
Normalized	9015	6	no crack	
		8	2.0 hr.	
Annealed	9015	8	0.7 hr.	
Normalized	Alloy No. 2	5	no crack	Atmosphere of 5% H_2 + 1% H_2O in argon
		5-1/2	no crack	
		6	0.7 hr.	
		7	0.2 hr.	
Normalized	Alloy No. 2	7	no crack	Atmosphere of 1% H_2O in argon
		8	2.3 hr.	
Annealed	Alloy No. 2	6	no crack	Atmosphere of 1% H_2O in argon
		7	1.1 hr.	

Welding conditions for XX10: 27V, 180 Amps, 8.5 in./min. 34.2 kji.
for XX15 and XX16: 22V, 200 Amps, 7.7 in./min. 34.2 kji.
for Alloy No. 2: 32V, 250 Amps, 15 in./min. 32.0 kji.

Table 8

Cracking Response of Single vs. Double Pass Welds

Lehigh restraint test of normalized HY-80 (Steel No. 1) welded with Alloy No. 2 electrode, DCRP, 250 amperes, 32 volts, 15 inches/minute, "wet" argon contains 1% H_2O, and "dry" argon is 99.95% pure and passed through desiccant just prior to welding.

Restraint	Single pass		Two pass wet argon	Two pass 1st wet argon 2nd dry argon	Two pass 1st dry argon 2nd wet argon
	Dry	Wet			
4"			no crack		
5"		no crack	7.0 hr.		
6"		2.5 hr.	1.5 hr.	no crack	no crack
6"				48 hr. crack	
7"		0.4 hr.			no crack
8"					6.5 hr.
8"	*no crack				

* 3 inch weld groove

Table 9

Spray vs. Drop Transfer

Lehigh restraint test welded with heat input of 32 kji and atmosphere of argon with 1% H_2O

Spray Transfer DCRP, 250 amperes, 32 volts, 15 in/min.		Drop Transfer DCRP, 190 amperes, 28 volts, 10 in/min.	Drop Transfer DCSP, 250 amperes, 32 volts, 15 in/min.
Restraint (ins)	Cracking Time	Cracking Time	Cracking Time
Navy HY-80*			
5-1/2			no crack
6-1/2			no crack
7	no crack		no crack
8	2.3 hr.	no crack	0.2 hr.
8 (3" bead)		1.0 hr.	
ASTM A212**			
6	no crack		
7	no crack		
7-1/2	0.8 hr.		no crack
8	no crack		no crack
8	0.7 hr.		0.34 hr.

* Steel No. 2, normalized condition welded with Alloy No. 2 electrode.
** Steel No. 10, as-rolled condition welded with Triple Deoxidized electrode on 3 inch groove by Kudva (44), not reported.

Table 10

Effect of Prior Heat Treatment on Crack Sensitivity

Lehigh restraint test of HY-80, welded with Alloy No. 2 electrode, DCRP, 250 amperes, 32 volts, 15 inches/minute, atmosphere of argon with 1% H_2O

Steel No. 2 (low chemistry 1 inch plate)

Restraint	Annealed	Spheroidized	Spray-Quenched and Tempered	Normalized	Spray Quenched
6"	no crack*	no crack			
7"	1.1 hr.	2.6 hr.	no crack	no crack	no crack
8"		3.0 hr.	0.45 hr.	2.3 hr.	no crack
8" (3" bead)					0.6 hr.

Steel No. 5 (high chemistry 1-1/2 inch plate)

5"			no crack	no crack	
5-1/2"			--------	0.5 hr.	
6"			0.5 hr.	0.7 hr.	

* Crack formed was smaller than critical (1/16" length) crack.

Table 11

Effect of Prior Heat Treatment on Hardness of Weld Metal and Heat Affected Zone in Low Chemistry HY-80 Steel

Vickers Diamond Pyramid with a 1 Kg load

	Specimen HYA2 Annealed			Specimen SQHA1 Spherodized			Specimen HN1 Normalized		Specimen QHB1 Spray Quenched	
				Heat Affected Zone						
	DPH	R_C	R_B	DPH	R_C	R_B	DPH	R_C	DPH	R_C
	439	44		439	44		426	43	439	44
	439	44		401	41		453	46	413	42
	413	42		439	44		426	43	439	44
	467	47		439	44		439	44	426	43
	426	43		426	43		439	44	439	44
	467	47		439	44				426	43
	413	42		426	43				439	44
	368	38		439	44					
Avg.	427	43.3		423	43.0		435	44.0	428	43.4
				Base Metal						
				189	8.2	89	276	27	413	42
Ferrite	159		81	182	6.5	87	283	28	426	43
	165	1.5	83	182	6.5	87	276	27	453	46
Carbide	330	33		182	6.5	.87			463	46
	305	30							426	43

Rockwell 30N converted to Rockwell "C"

	Weld Metal			
	37	36	37	30
	37	36	37	36
	38	35	37	34
	36	35	36	36
	36	35	37	36
	36	35	36	36
Avg.	36.8R_C	35.4R_C	36.8R_C	34.7R_C

Table 12

Effect of Compositional Changes on Delayed Cracking of HY-80 Steel

Lehigh restraint test of normalized specimens welded with Alloy No. 2 electrode, DCRP, 250 amperes, 32 volts, 15 inches/minute, atmosphere of argon with 1% H_2O (except as indicated)

Steel No.	2	4	1	5	3
Restraint (ins.)	1" Low Chem.	1" Vacuum Melted High Chem.	1" High Chem.	1-1/2" High Chem.	1" High Chem. with 0.003% Rare Earths Added
5"			no crack	no crack*	no crack
5-1/2"				0.5 hr.	
6"		no crack	2.6 hr.	0.7 hr.	0.6 hr.
7"	no crack	no crack	0.4 hr.		
8"	2.3 hr.	1.3 hr.			
Dry Argon Atmosphere					
8"	no crack	no crack (3" groove)	no crack (3" groove)	no crack (3" groove)	no crack

* Two tests

Table 13

Effect of Plate Composition on Cracking Response

Lehigh restraint test welded with Alloy No. 2 electrode, DCRP, 250 amps, 32v, 15 inches/minute, atmosphere of argon with 1% H_2O

Steel No. → / Restraint (ins.)	6	9	2	7	10	1	11
	HY-65	A203	HY-80	T-1	A212	HY-80	A302
3							no crack
4							4.1 hr.
5				no crack	no crack	no crack	0.23 hr.
6				8.2 hr.	4.5 hr.	2.5 hr.	0.23 hr.
7		no crack	no crack	1.3 hr.	2.0,0.8 hr.	0.4 hr.	
8	no crack	no crack	2.3 hr.	3.2,3.6 hr.	1.2 hr.		
8 (3" bead)	1.8 hr.	5.6,0.7 hr.					
C. Equiv. (B) =	0.40	0.55	0.54	0.53	0.56	0.61	0.67
C. Equiv. (C) =	0.35	0.49	0.50	0.46	0.50	0.55	0.61
C. Equiv. (W) =	0.31	0.44	0.47	0.38	0.44	0.54	0.49

Battelle formula = (B)=% (C + Mn/4 + Si/4 + Cr/10 + Ni/20 + Cu/40 - Mo/50 - V/10)
Corrected Winterton = (C) = % (C + Mn/4 + Cr/10 + Ni/20 + Cu/40 - Mo/50 - V/10)
Winterton formula = (W) = % (C + Mn/6 + Cr/10 + Ni/20 + Cu/40 - Mo/50 - V/10)

HY-65 and HY-80 steels were normalized. A203, A212 and A302 steels were as-rolled. A212 exhibited banding. "T-1" steel was quenched and tempered. Steels 1, 2 & 11 cracked in HAZ.

Table 14

Effect of Electrode Composition on Crack Susceptibility

Lehigh restraint test welded with DCRP, 250 amps, (except as noted), DCRP, atmosphere of argon with 1% H_2O

Steel No. 7 ("T-1"), quenched and tempered

Restraint	Triple Deox.	Alloy No. 1	Alloy No. 2	Alloy No. 3	Pure Iron
4"	no crack				
5"	1.2 hr.	no crack	no crack	no crack	no crack
6"	--	13.6 hr.	8.2 hr.	1.8 hr.	no crack
7"	--	3.0 hr.	1.3 hr.	5.0 hr.	no crack
8"	--	9.6 hr.	3.2,3.6 hr.	--	no crack
8" (3" bead)	--	--	--	--	no crack
8" (3" groove)	--	--	--	--	0.3 hr.

Steel No. 11 (ASTM A-302), as rolled

	Argon with 1% H_2O				Dry Argon Atmosphere*	
Restraint	Triple Deox.	Pure Iron	Alloy No. 2	310-SS (25-20)	Triple Deox.	Alloy No. 2
2-1/2"	no crack	--	--	--	no crack	--
3"	7.2 hr.	no crack	no crack	--	55 hr.	no crack
4"	0.5 hr.	0.6 hr.	4.1 hr.	no crack	34 hr.	24 hr.
4-1/2"	--	0.4 hr.	--	--	--	--
5"	0.5 hr.	0.3 hr.	0.2 hr.	no crack	--	--
6"	--	--	0.2 hr.	no crack	27 hr.	16 hr.
7"	--	0.2 hr.	--	hot crack	--	--
8"	--	--	--	--	1.5 hr.	15 hr.

Table 14 (Continued)

Steel No. 5 (1-1/2 inch HY-80), normalized

	Argon with 1% H_2O	
Restraint	Pure Iron	Alloy No. 2
5"	---	no crack, no crack
5-1/2"	---	0.5
6"	---	0.7
8" (3" groove)	no crack	---

* Work by Kudva (44)

Table 15

Locus of Delayed Crack Initiation in Various Studies

Lehigh restraint tests welded at 250 amps

Base Plate	Electrode	Atmosphere	Restraint	Locus of Crack
A212 (Steel No 10)	Alloy No. 2	1% H_2O in argon	6 to 8"	weld metal
	Triple deox.	1% H_2O in argon	8"(3" bead)	HAZ
A203 (Steel No. 9)	Alloy No. 2	1% H_2O in argon	8"	weld metal, fusion line
HY-65 (Steel No. 6)	Alloy No. 2	1% H_2O in argon	8"	weld metal
T-1 (Steel No. 7)	Alloy No. 2	1% H_2O in argon	6-8"	fusion line
	Triple deox.	1% H_2O in argon	4" (microcrack)	HAZ
A302 (Steel No. 11)	Pure iron*	1% H_2O in argon	4"	HAZ
	Triple deox.	1% H_2O in argon	3"	HAZ
	Alloy No. 2	1% H_2O in argon	4"	HAZ
	310-SS	1% H_2O in argon	8"	hot cracks in weld metal
Low chem HY-80 (Steel No. 2)	Alloy. No. 2	1% H_2O in argon	8" (3" bead)	weld metal, fusion line
		1% H_2O in argon	8"	fusion line, HAZ

Table 15 (Continued)

Base Plate	Electrode	Atmosphere	Restraint	Locus of Crack
Low-chem HY-80 (Steel No. 2)	Alloy No. 2			
		5% H_2 + 1% H_2O in argon	6"	HAZ
		5% H_2 + 1% H_2O in argon	7"	fusion line, HAZ
		5% H_2 in argon	6"	fusion line, HAZ
	Coated electrodes	-------	6-8"	fusion line, HAZ
High chem HY-80 (Steel No. 1)	Alloy No. 2	1% H_2O in argon	5"**	HAZ
		1% H_2O in argon	6"	HAZ
				HAZ
Rare earth HY-80 (Steel No. 3)	Alloy No. 2	1% H_2O in argon	6"	HAZ
vac. melt HY-80 (Steel No. 4)	Alloy No. 2	1% H_2O in argon	8"	HAZ
1-1/2" high chem HY-80 (Steel No. 5)	Alloy No. 2	1% H_2O in argon	5-1/2"	fusion line

* Welded at 300 amps
** Double pass weld: 1st pass "wet", 2nd pass "wet"

Table 16

Hardness Survey of Coarse Grained Heat Affected Zone Areas

Metallographic sections taken from restraint specimens of 1 inch steel plates. Vickers Diamond Pyramid Hardness (DPH) using 1 Kg load.

		Averages
Specimen A3- ASTM A-302 Steel		
Vickers DPH	467, 533, 515, 533, 551, 515, 533, 453, 498, 515, 482	505
Equivalent Rockwell "C"		49.4
Specimen Y-1 - Navy HY-80 (Steel No. 1)		
Vickers DPH	426, 439, 426, 426, 439, 439, 413, 413, 426, 426, 426, 378	426
Equivalent Rockwell "C"		43.2
Specimen PR10 - "T-1" Steel		
Vickers DPH	413, 413, 426, 413, 413, 426, 453, 413, 401, 390, 476, 413	420
Equivalent Rockwell "C"		42.7
Specimen ER6 - ASTM A-203 Steel		
Vickers DPH	305, 348, 358, 313, 330, 313, 348, 330, 297, 330	325
Equivalent Rockwell "C"		32.8
Specimen GN6 - Navy HY-65 Steel		
Vickers DPH	276, 251, 261, 263, 330, 330, 263, 401, 269, 439, 283	297
Equivalent Rockwell "C"		29.4
Specimen BR23 (1st four readings) and BR22 (balance of readings) ASTM A-212 Steel		
Vickers DPH	263, 297, 251, 283, 251, 229, 219, 251, 283, 269, 330, 290, 290, 339, 439	287
Equivalent Rockwell "C"		28.1

Table 17

Hardness Survey of Weld Metal Deposits

Metallographic sections taken from restraint specimens of 1 inch steel plates.

		Averages
1.	Specimen A7 - Triple deox. electrode on A-302 plate	
	Rockwell 30N 51.0, 50.0, 50.0, 49.5, 53.0, 53.5, 51.0, 51.5, 50.0	51.1
	Equivalent Rockwell "C"	30.8
	Equivalent Vickers DPH	308
2.	Specimen A3 - Alloy No. 2 electrode on A-302 plate	
	Rockwell 30N 57.5, 58.5, 58.5, 59.0, 55.0, 60.5, 60.5, 60.0, 59.5, 60.0	58.9
	Equivalent Rockwell "C"	39.4
	Equivalent Vickers DPH	386
3.	Specimen P10 - Alloy No. 2 electrode on "T-1" plate	
	Rockwell 30N 56.0, 55.0, 57.0, 57.0,57.0, 56.0, 56.0, 55.5	56.2
	Equivalent Rockwell "C"	36.4
	Equivalent Vickers DPH	358
4.	Specimen Y1 - Alloy No. 2 electrode on high chem HY-80 plate	
	Rockwell 30N 55.5, 55.5, 56.5, 53.5, 54.0, 56.0, 57.0, 57.0, 57.0, 56.5	55.9
	Equivalent Rockwell "C"	36.0
	Equivalent Vickers DPH	355
5.	Specimen ER6 - Alloy No. 2 electrode on ASTM A-203 plate	
	Rockwell 30N 54.5, 53.5, 53.5, 55.5, 52.5, 56.0, 55.0, 53.0, 54.5, 56.0	54.4
	Equivalent Rockwell "C"	34.4
	Equivalent Vickers DPH	340
6.	Specimen GN6 - Alloy No. 2 electrode on Navy HY-65 plate	
	Rockwell 30N 50.0, 52.0, 51.0, 50.0, 50.0, 52.0, 52.0, 51.5, 48.0, 53.5, 49.0, 52.5	51.0
	Equivalent Rockwell "C"	30.6
	Equivalent Vickers DPH	307
7.	Specimen BR31 - Alloy No. 2 electrode on ASTM A-212 plate	
	Rockwell 30N 51, 54, 54, 54, 54, 54, 53, 54, 53, 54	53.5
	Equivalent Rockwell "C"	33.5
	Equivalent Vickers DPH	332

Table 17 (Continued)

		Averages
8.	Specimen PR17 - Triple deox. electrode on "T-1" plate	
	Rockwell 30N 50.5, 51.0, 50.5, 50.5, 52.0, 51.0, 52.0, 52.0, 51.0, 52.0	51.3
	Equivalent Rockwell "C"	31.0
	Equivalent Vickers DPH	310

Table 18

Delayed Cracking in Low Hardenability Steels

Lehigh restraint tests welded at 250 amperes, DCRP

Restraint	Argon Atmosphere Additions	Travel (in/min)	Cracking Time	Did HAZ* Contain Martensite?	Were* Microcracks Present?
A201 (Steel No. 8)					
Alloy No. 2 electrode					
8 (3" groove)	1% H_2O	15	no crack	---	---
8 (3" groove)	1% H_2O + 5% H_2	15	no crack	---	---
8 (1" groove)	1% H_2O + 5% H_2	15	no crack	no	no
Triple deox. electrode					
8 (3" groove)	1% H_2O	6	no crack	no	no
8 (3" groove)	1% H_2O + 5% H_2	15	no crack	---	---
A212 (Steel No. 10)					
Alloy No. 2 electrode					
5	1% H_2O	15	no crack	yes	yes, in weld
6	1% H_2O	15	4.5 hr.	---	---
7	1% H_2O	15	0.7, 2.0 hr.	---	---
8	1% H_2O	15	1.2, 2.6 hr.	---	---
Triple deox. electrode					
8	1% H_2O	15	no crack	---	---

Table 18 (Continued)

Restraint	Argon Atmosphere Additions	Travel (in/min)	Cracking Time	Did HAZ* Contain Martensite?	Were* Microcracks Present?
Triple deox. electrode					
8 (3" bead)	1% H_2O	6	12.8 hr.	yes	---
8 (3" bead)	1% H_2O	15	1.0 hr.	yes	---

* Did examination with the light microscope reveal any microcracks, or martensite?

Table 19

Hardness Inspection of Weldments on ASTM A-201 at Two Heat Input Levels

Metallographic sections from Lehigh restraint tests

Specimen No. A201-1, 250 amps, 6 in/min, 3" weld, triple deox. electrode						Specimen No. A201-3, 250 amps, 15 in/min, 1" weld, Alloy No. 2 electrode					
Vickers DPH (1 Kg load)	Equivalent Rockwell "C"	Equivalent Rockwell "B"	Rockwell 30N	Equivalent Rock. "B"	Vic. DPH	Vickers DPH (1 Kg load)	Equivalent Rockwell "C"	Equivalent Rockwell "B"	Rockwell 30N	Equivalent Rock. "C"	Vic. DPH
Heat Affected Zone											
189	8	89				224	17	96			
193	9	90				219	16	95			
168		89				239	20	98			
175	5	86	- low reading			234	19	97			
186	8	89				276	27	103			
178	5	87				297	29	105	- low reading		
189	9	90				269	25	102			
189	8	89				201	11	92	- low reading		
201	11	92									
214	14	94	- high reading								
214	14	94									
210	13	93									
205	12	92									
193		90.0	Averages			242	20.7	98.4			
Weld Metal											
210	13	93	79	95	220	257	24	101	49	29	290
197	10	91	79	95	220	263	25	101	50	30	298
193	9	90	80	96	226	283	27	104	50	30	298
193	9	90	78	93	208	276	27	103	49	29	290
178	5	87	78	93	208				51	30	307
182	7	88	78	93	208						
193 Avg.		90.1	Avg.	94.1	214	269	25.4	102	Avg.	29.6	298

Table 19 (Continued)

Specimen No. A201-1				Specimen No. A201-3		
	Rockwell 30N	Equivalent Rock. "B"	Vic. DPH	Rockwell 30T	"B"	Equivalent DPH
			Base Metal			
	65	72	132			
	67	75	140	58	62	110
	62	68	123	60	65	117
	62	68	123	56	59	105
	66	74	137	59	64	115
	68	77	145	56	59	105
	68	77	145	60	65	117
	69	78	148	57	61	108
Averages		73.6	136		62.1	110

Table 20

Delayed Cracking Tests on Maraging Steel

Lehigh restraint test of Steel No. 12, 1" plate, 8 inch restraint, 3 inch groove and weld, DCRP, 250 amperes, 32 volts, 15 inches/minute, atmosphere of 5% H_2 + 1% H_2O in argon

Plate Heat Treatment	Electrode	Cracking
Annealed*	18% Ni Maraging	no crack
	Alloy No. 2	no crack
Maraged**	18% Ni Maraging	no crack

* Solution treated at 1500°F, 1 hour, air cooled

** Solution treatment followed by maraging at 900°F, 3 hours, air cooled

Table 21

Retained Austenite Measurements

All welds were made using Alloy No. 2 electrode at 250 amps, 15 inches/minute travel, and an atmosphere of argon with 1% H_2O. Heat treatments indicated pertain to the base metal of Lehigh restraint specimens.

	Percent Retained Austenite
1. Steel No. 5 - high chemistry HY-80, 1-1/2" plate, quenched and tempered	
Base metal	0.0
Heat affected zone	1.2
2. Steel No. 2 - low chemistry HY-80, 1" plate	
Normalized base metal	2.0
Heat affected zone	0.66
Heat affected zone (1% H_2O + 5% H_2)	0.24
Annealed base metal	0.61
Heat affected zone	1.25
3. Steel No. 11 - ASTM A302, 1" plate	
As-rolled base metal	0.2
Heat affected zone	1.0
Weld metal (Alloy No. 2)	1.2

Figure 1

Base Metal Microstructures

Base Metal Microstructures

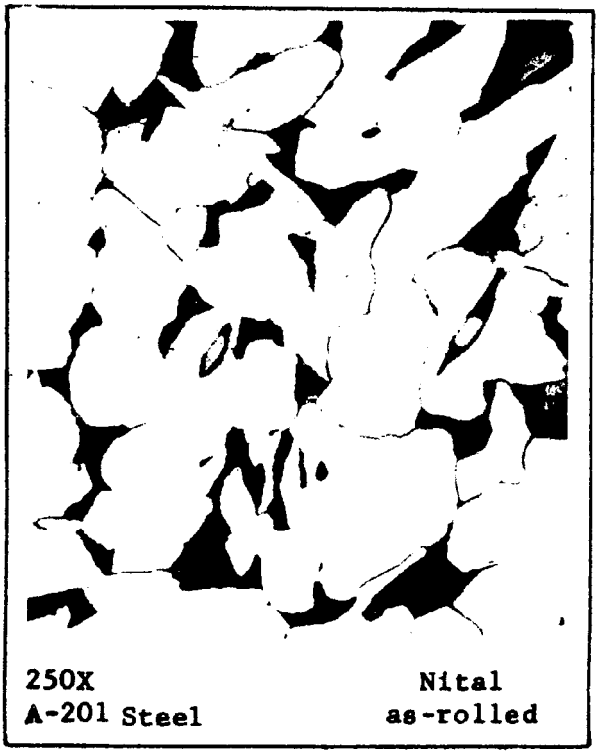

250X Nital
A-201 Steel as-rolled

250X Nital
A-212 Steel as-rolled

250X Nital
A-203 Steel as-rolled

500X Nital
A-302 Steel as-rolled

Base Metal Microstructures (Continued)

500X Nital
"T-1" Steel, quenched & tempered

500X Nital
HY65 Steel normalized

250X
Etchant: 50ml HCl, 25ml HNO_3, 1g $CuCl_2$, 150ml H_2O

18% Nickel Maraging
Solution Treated

250X
Etchant: 50ml HCl, 25ml HNO_3, 1g $CuCl_2$, 150ml H_2O

18% Nickel Maraging
Maraged Condition

Figure 2

Effect of Prior Heat Treatment on Minimum Restraint Level Required to Crack Low Chemistry HY-80

Figure 2

Effect of Prior Heat Treatment on Minimum Restraint Level Required to Crack Low Chemistry HY80

Lehigh restraint test of 1"plate welded with No. 2 electrode on 5" groove with 5" bead (except as indicated) at 250 amperes and 15"/minute travel in water-saturated argon. (Photographs at 500X, nital etch)

As-quenched 1650°F
Cracked in 0.6 hr at
8"Restraint (3"bead)

Normalized 1650°F
Cracked in 2.3 hr
at 8" Restraint

Quenched 1650°F
Tempered 1250°F, 1 1/2 hrs
Cracked 0.4 hr at 8"Restraint

Quenched 1650°F
Spheroidized 1250°F, 36 hrs
Cracked in 2.6 hr at 7"Restraint

Furnace cooled
from 1650°F

Cracked in 1.1 hr
at 7" Restraint

Figure 3

Apparatus

A - Welding Bed
B - Side view of Microformer on specimen
C - Crack Detection Unit
D - Hydrogen Evolution Apparatus
E - Postheating Strips
F - Postheater with Specimen

Apparatus

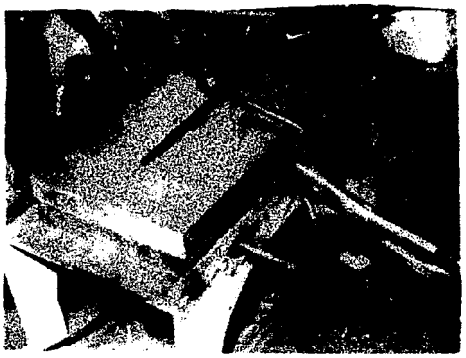

A - Welding Bed

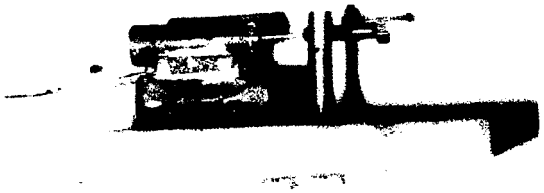

B - Side view of microformer on specimen

C - Crack Detection Unit

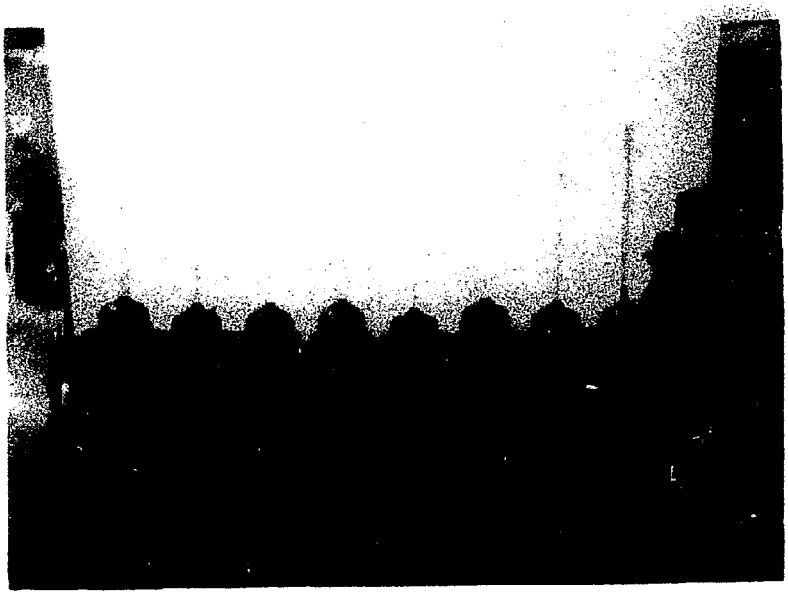

D - Hydrogen Evolution Apparatus

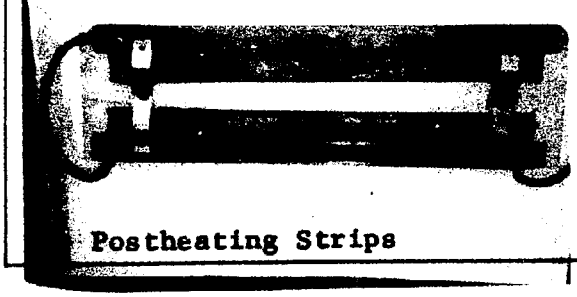

Postheating Strips

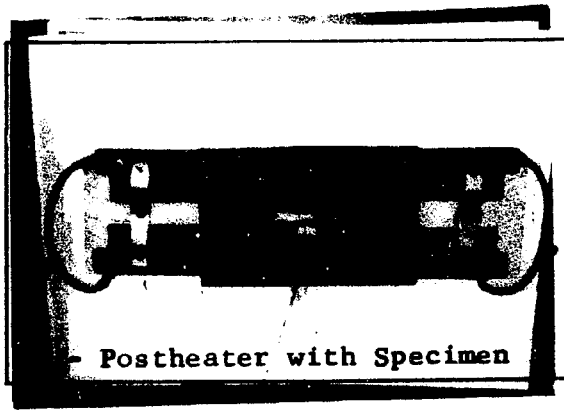

Postheater with Specimen

Figure 4

Lehigh Restraint Specimen

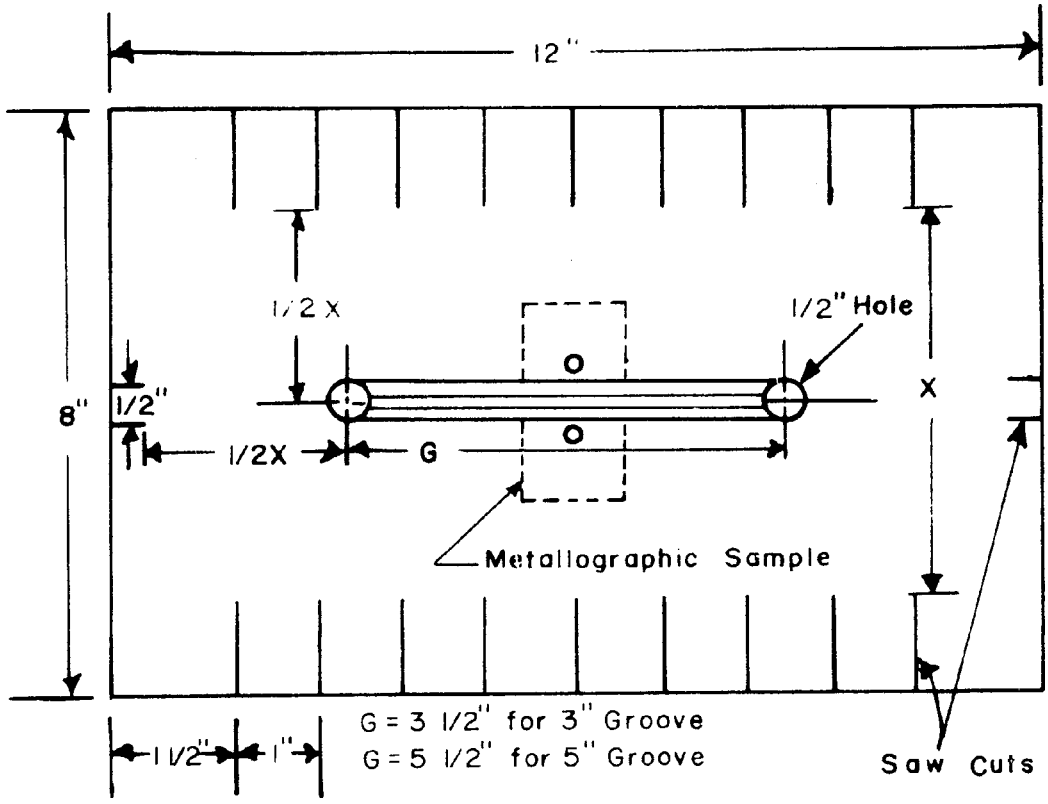

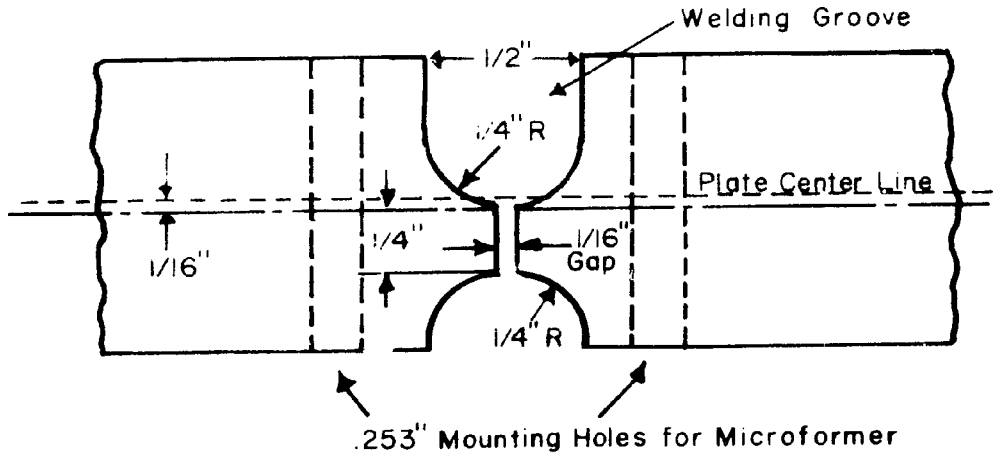

Lehigh Restraint Specimen

Figure 5

Schematic of Microformer on Specimen

Schematic of Microformer on Specimen

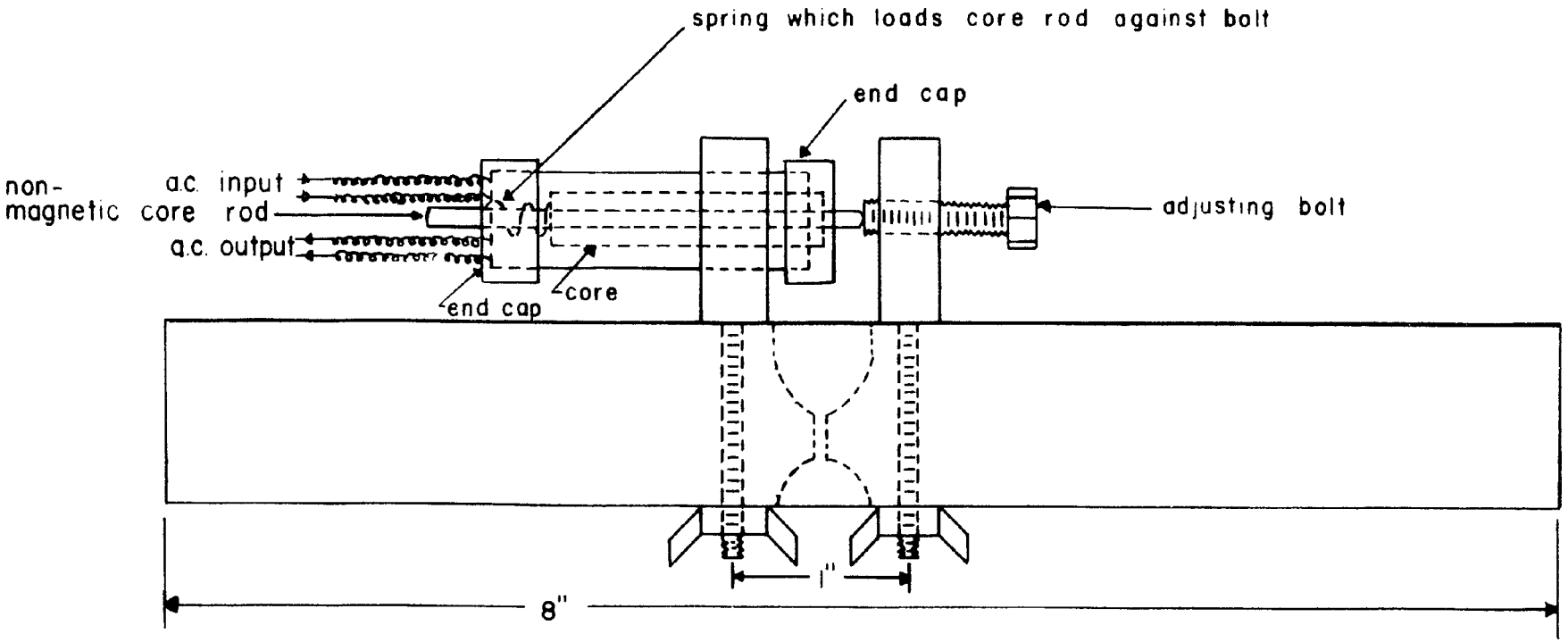

Figure 6

Schematic of Microformer with Rectifier Circuit

Schematic of Microformer with Rectifier Circuit

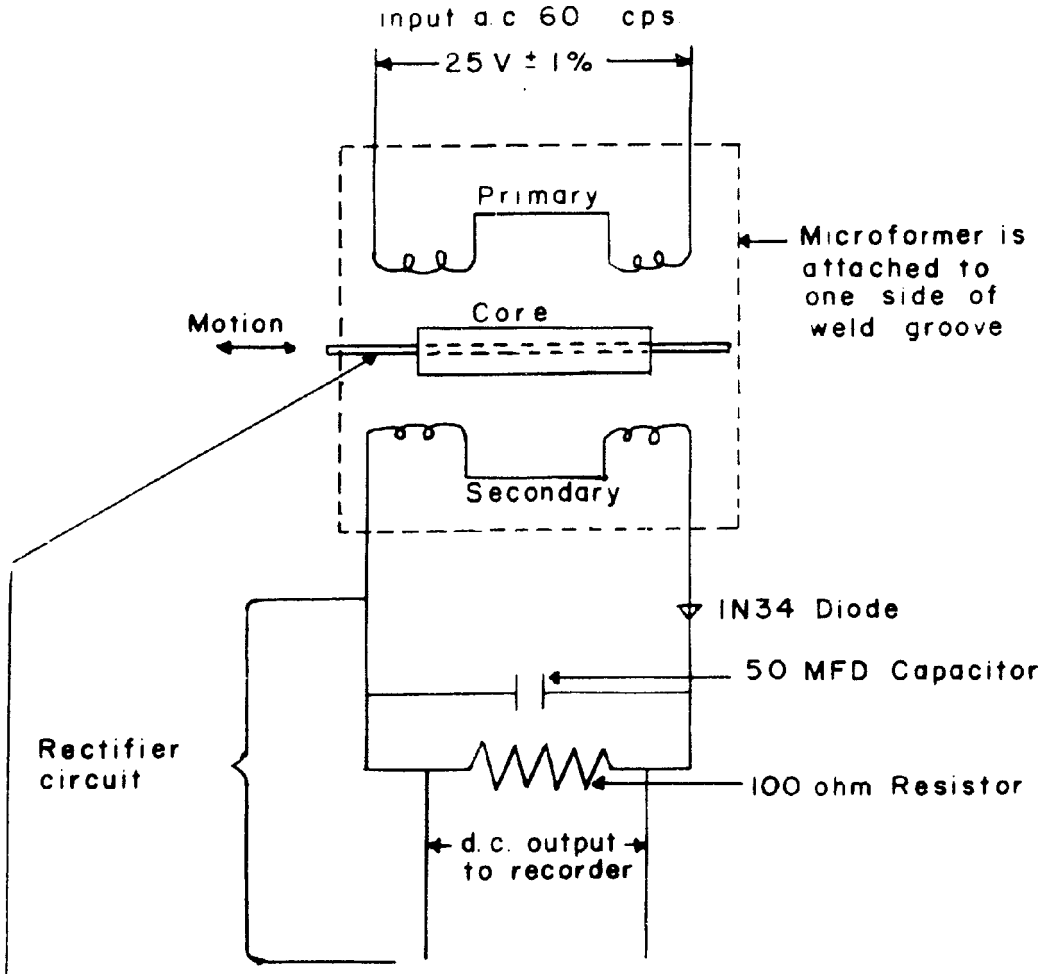

Core rod is spring loaded against fitting attached to opposite side of weld groove.

Note: Microformer a.c. output rated at 4.6 mv/0.001" core displacement.

Figure 7

Schematic of Crack Detection Circuit

Schematic of Crack Detection Circuit

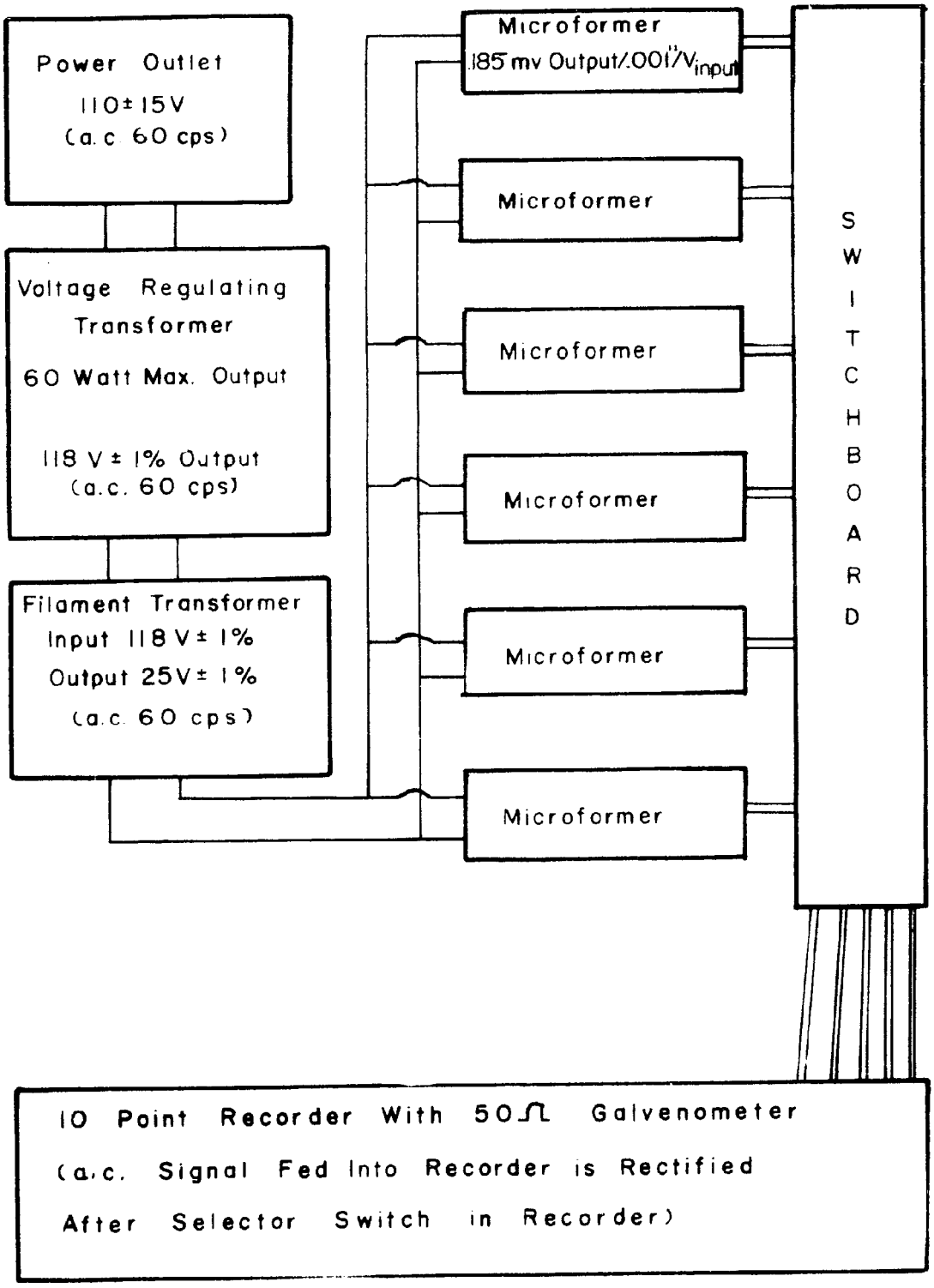

Figure 8

Crack Susceptibility as a Function of Hydrogen Content for Low Chemistry HY-80 Steel Welded with Alloy No. 2 Electrode

Crack Susceptibility as a Function of Hydrogen Content For Low Chemistry HY-80 Steel Welded With Alloy No. 2 Electrode

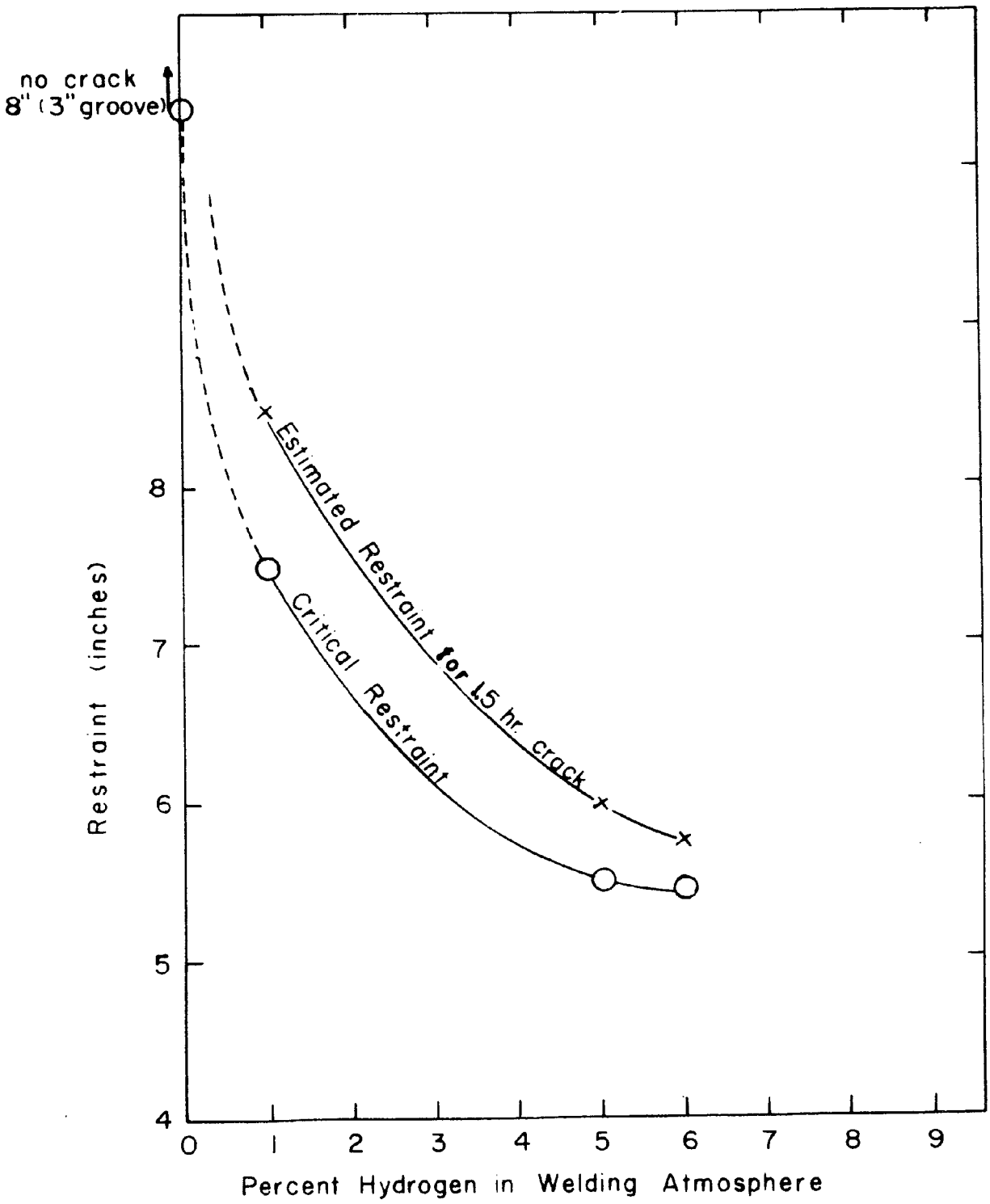

Figure 9

Cracking Time as a Function of Reciprocal of Restraint

Cracking Time as a Function of Reciprocal of Restraint

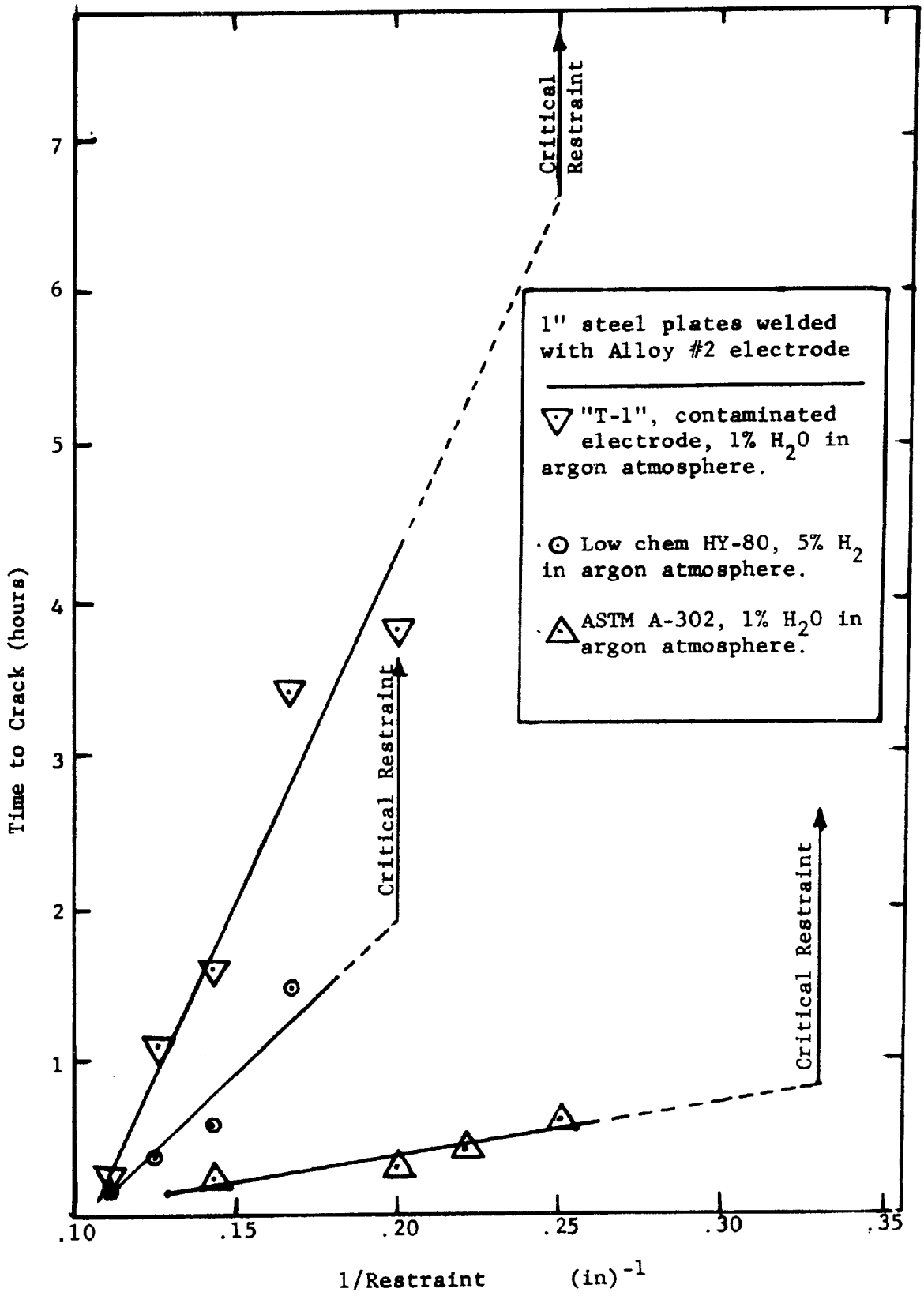

Figure 10

Effect of Hydrogen on Cracking Time of Low Chemistry
HY-80 at 8" Restraint Welded with Alloy No. 2 Electrode

Effect of Hydrogen on Cracking Time of Low Chem HY80 at 8" Restraint welded with Alloy NO. 2 Electrode

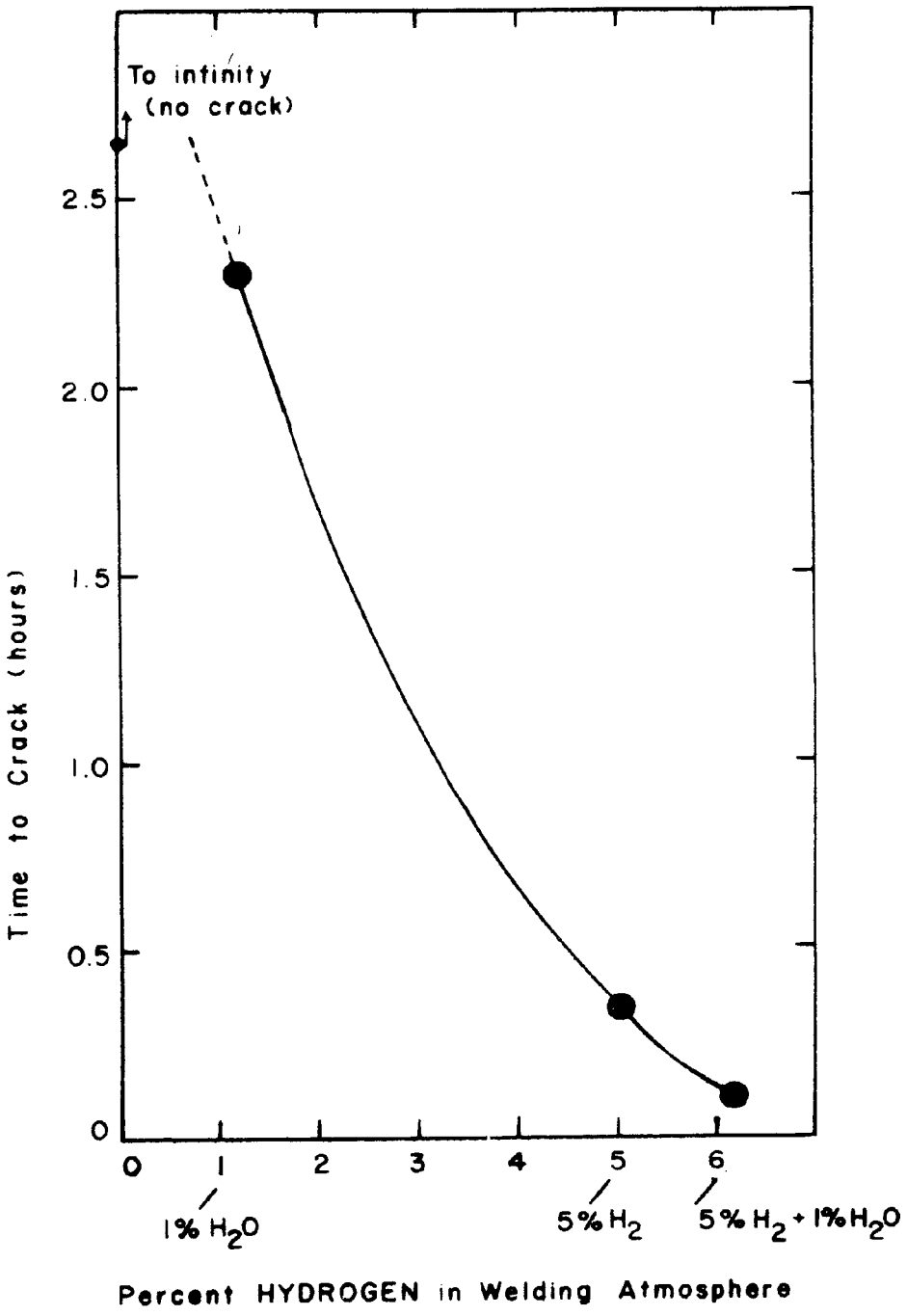

Figure 11

Model for Hydrogen Diffusion in Weldments

A - Escape from charged bead

B - Competitive diffusion process

C - Comparison of "wet" and "dry" beads

MODEL FOR HYDROGEN DIFFUSION IN WELDMENTS

Figure A - Escape from charged bead

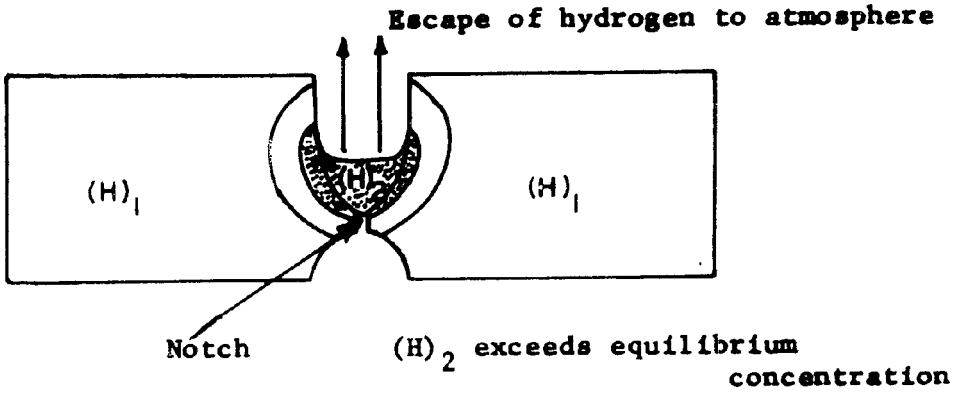

Figure B - Competitive diffusion process

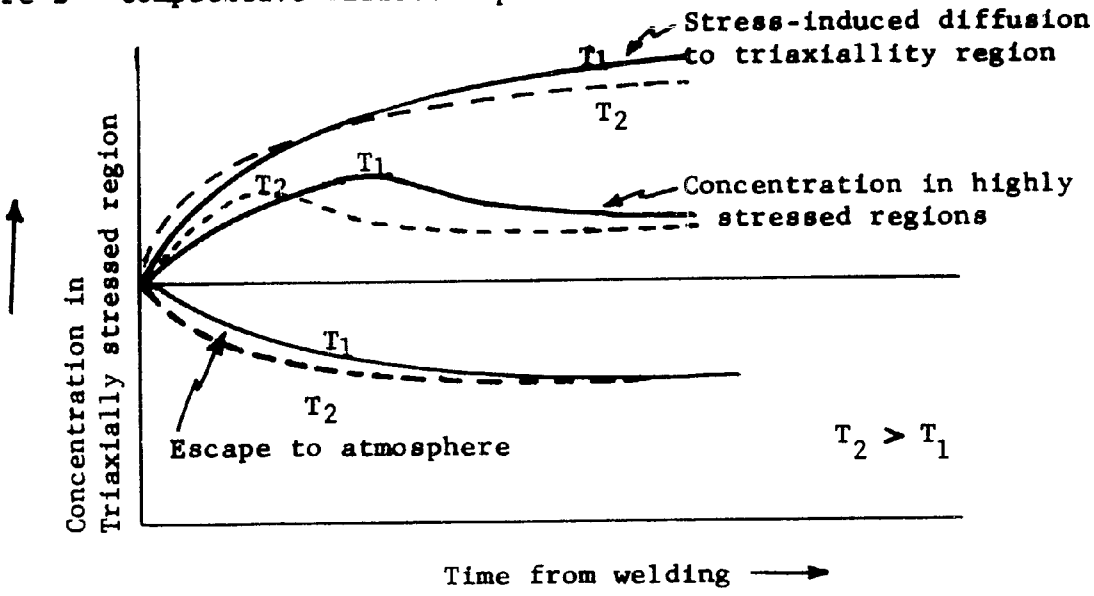

Figure C - Comparison of "wet" and "dry" beads

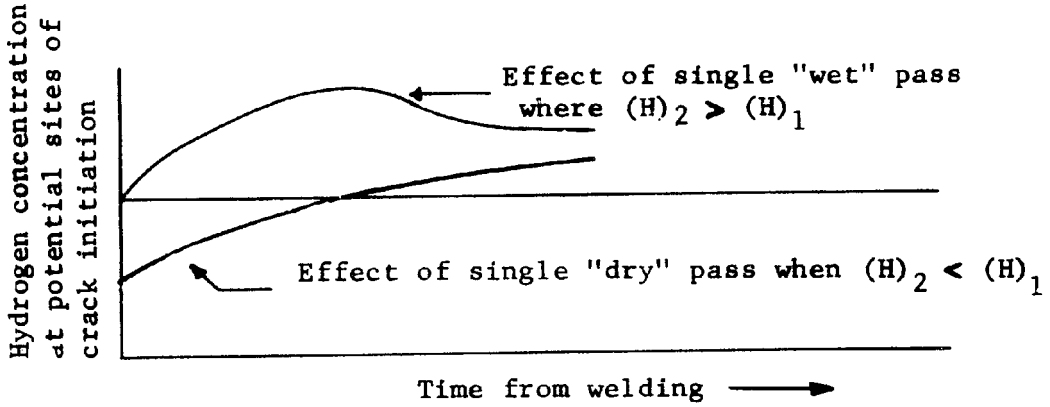

Figure 12

Postheating of "T-1" Steel

Postheating of "T-1" Steel

Lehigh Restraint Test Welded With Alloy No. 2 Electrode
at 250 Amperes, 32 Volts in Atmosphere of Argon + 1% H_2O

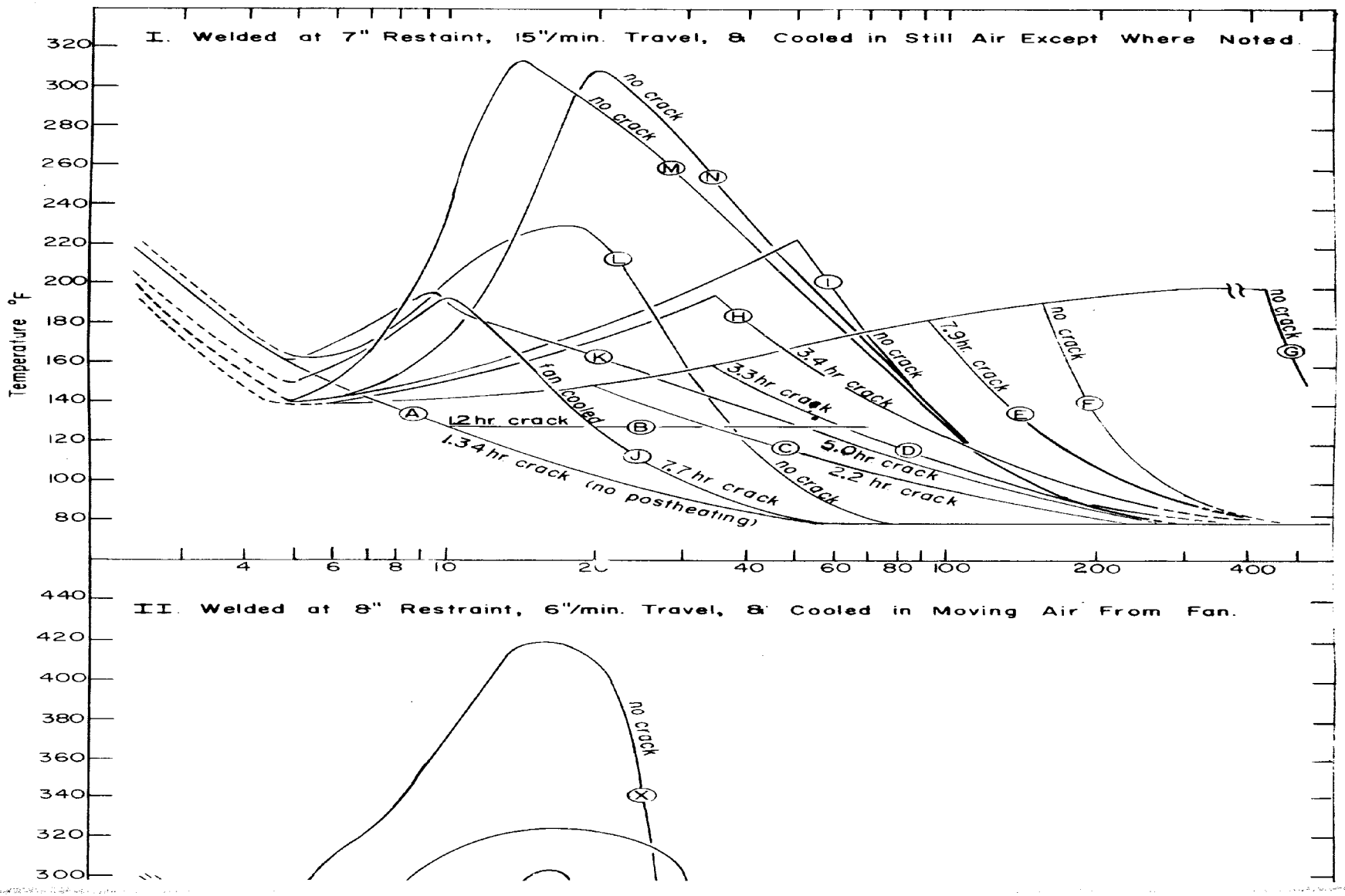

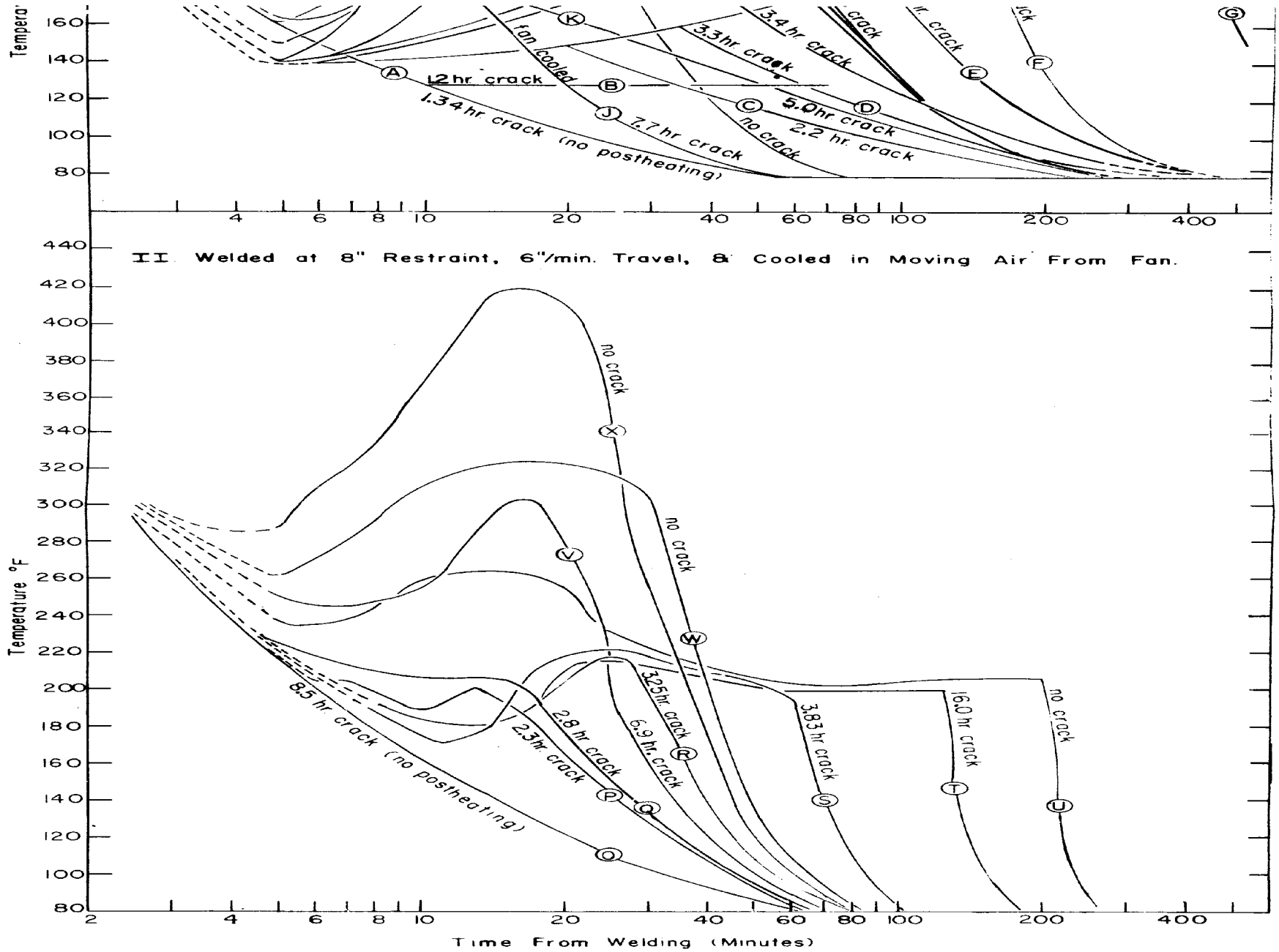
Tempera
160
140
120
100
80
4
6
8
10
20
40
60
80
100
200
400
A
1.2 hr. crack
1.34 hr. crack (no postheating)
fan cooled
B
J
7.7 hr. crack
C
no crack
3.3 hr. crack
3.4 hr. crack
5.0 hr. crack
2.2 hr. crack
D
E
F
G
K
II Welded at 8" Restraint, 6"/min. Travel, & Cooled in Moving Air From Fan.
Temperature °F
440
420
400
380
360
340
320
300
280
260
240
220
200
180
160
140
120
100
80
2
4
6
8
10
20
40
60
80
100
200
400
Time From Welding (Minutes)
no crack
X
no crack
W
V
8.5 hr. crack (no postheating)
2.3 hr. crack
2.8 hr. crack
P
Q
O
3.25 hr. crack
6.9 hr. crack
R
3.83 hr. crack
S
16.0 hr. crack
T
no crack
U

Figure 13

Arrhenius Plot of Uncorrected Cracking Data

ARRHENIUS PLOT OF UNCORRECTED CRACKING DATA

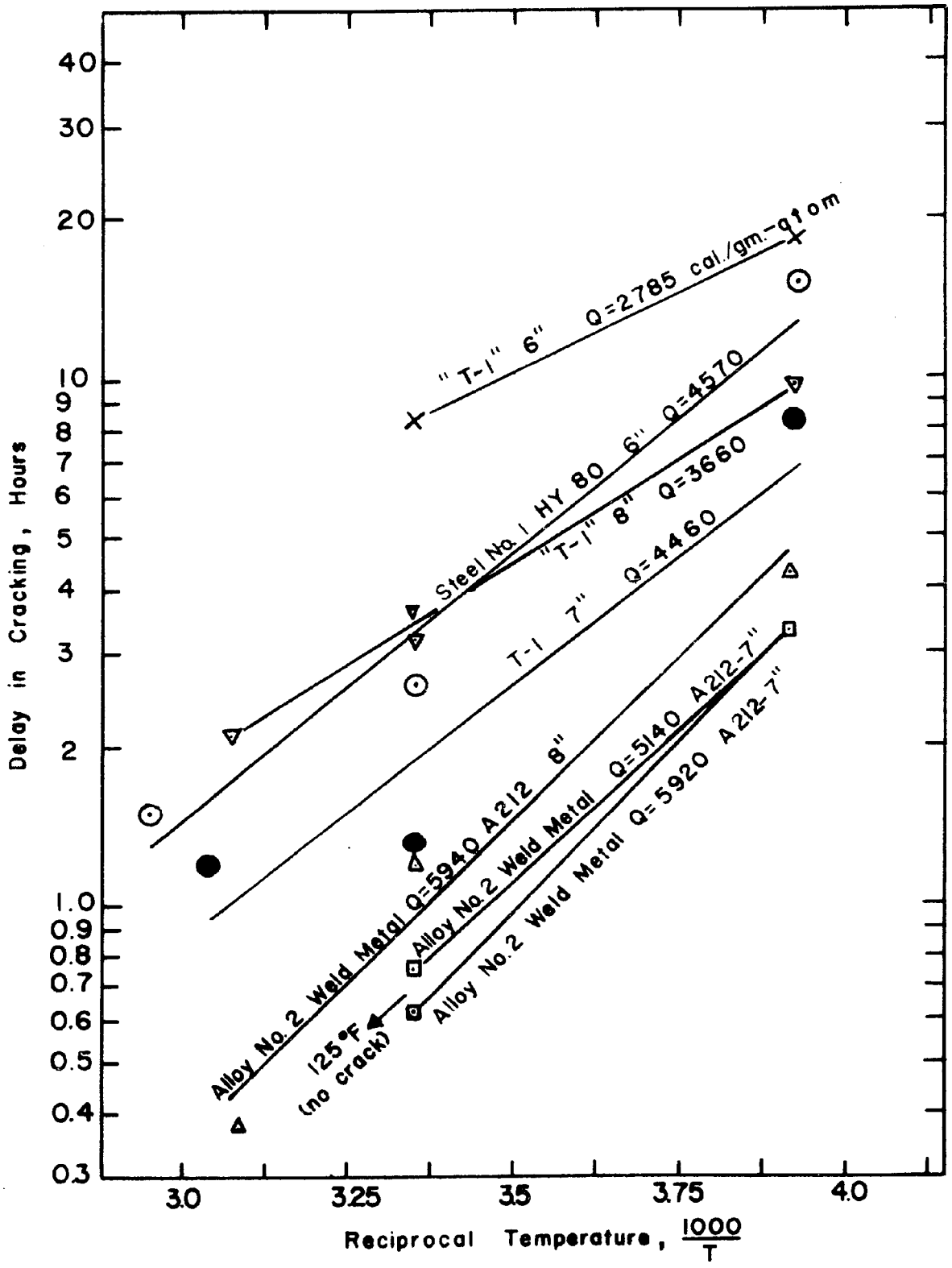

Figure 14

Arrhenius Plot of Corrected Cracking Data

ARRHENIUS PLOT OF CORRECTED CRACKING DATA

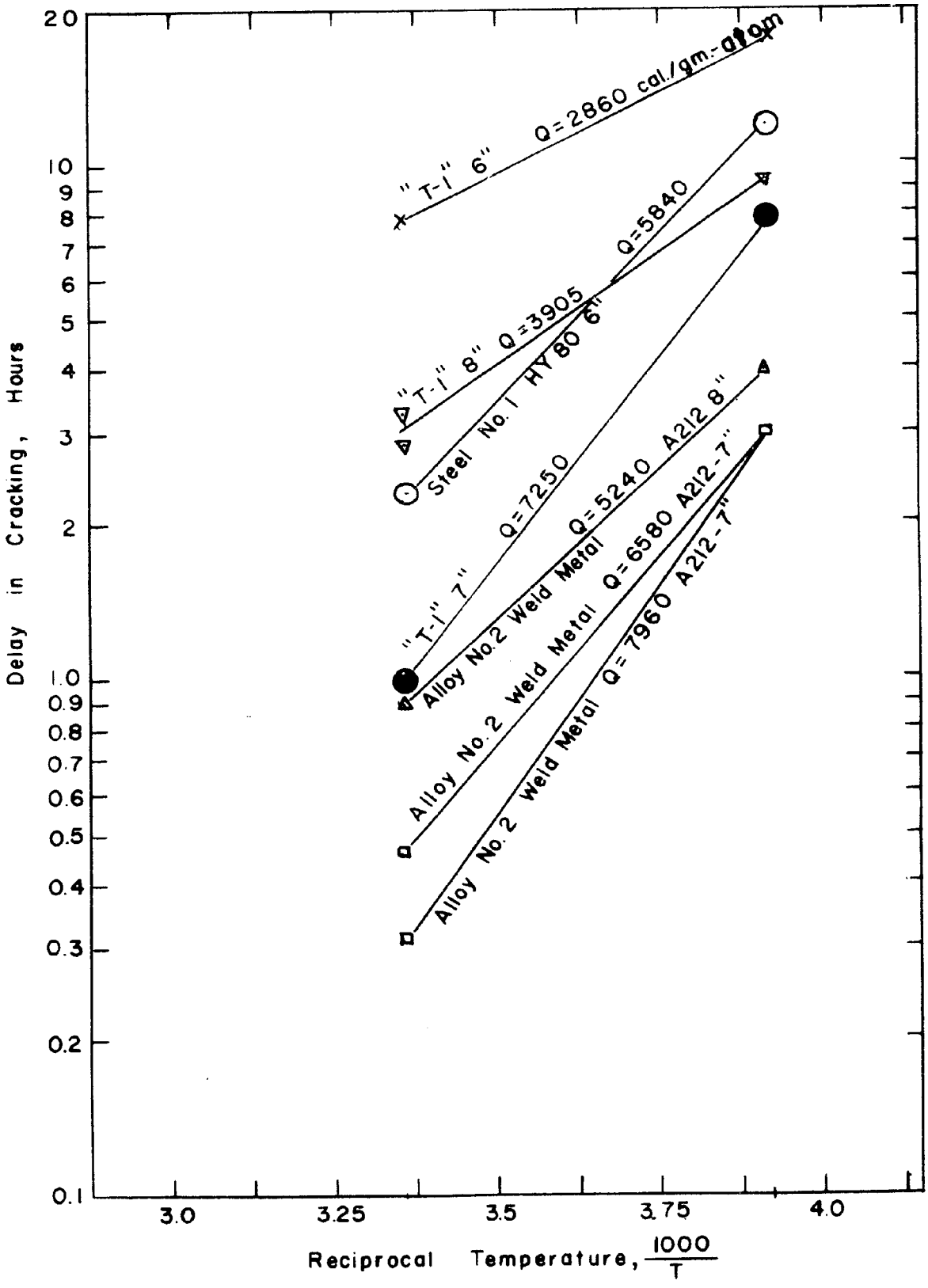

CALCULATED 1 HOUR POSTHEATING TEMPERATURES REQUIRED TO PREVENT CRACKING OF "T-1" STEEL WELDED WITH ALLOY NO. 2 ELECTRODE AS A FUNCTION OF BEAD SIZE

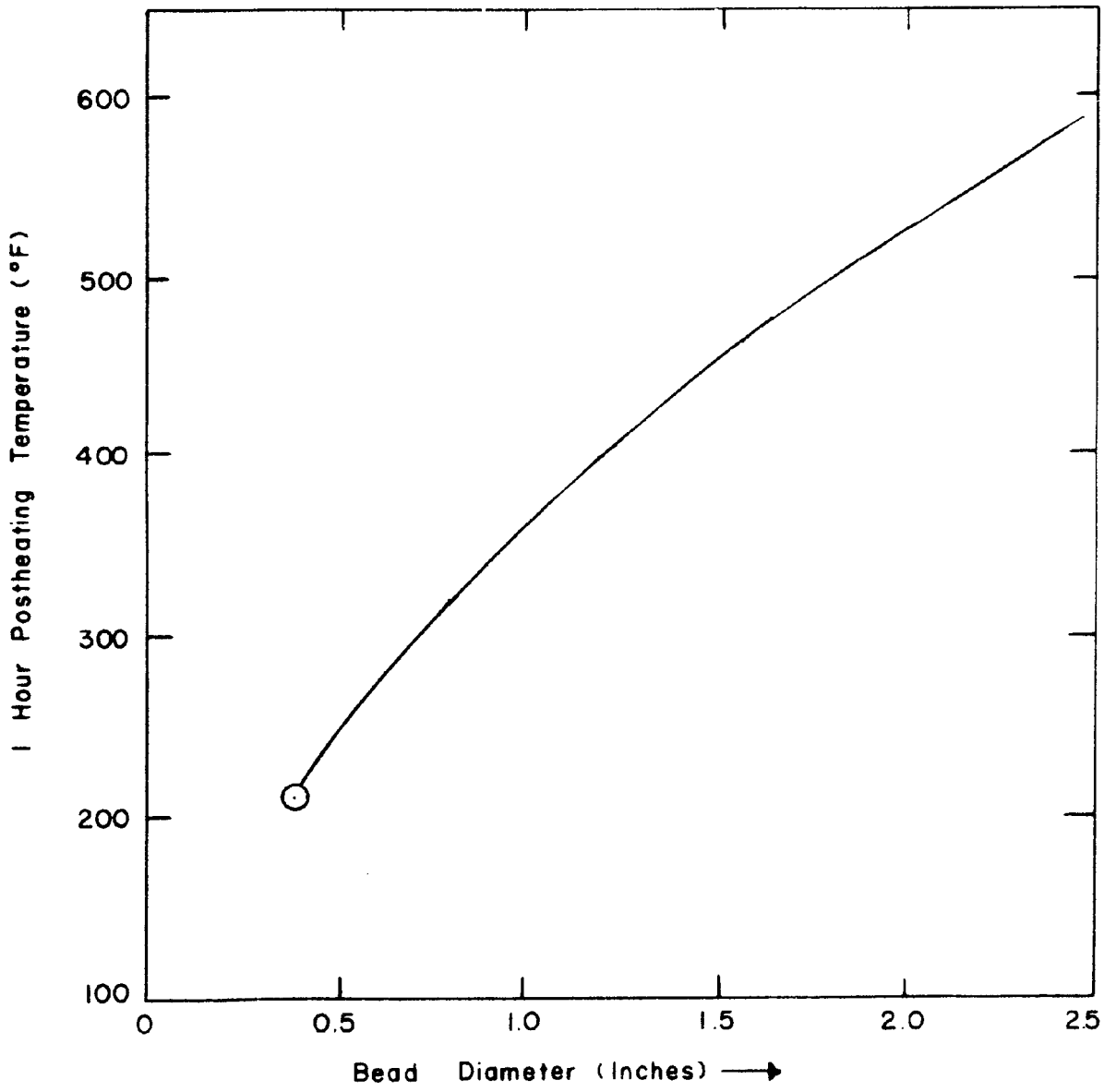

Figure 15

Calculated 1 Hour Postheating Temperatures Required to Prevent Cracking of "T-1" Steel Welded with Alloy No. 2 Electrode, as a Function of Bead Size

Figure 16

Effect of Base Metal on Crack Initiation

Figure

Effect of Base Metal on Crack Initiation

Lehigh restraint test of 1-inch plate welded with No. 2 electrode on 5-inch groove at 6 inches restraint with 5-inch bead at 250 amperes, 15 inches per minute travel in water saturated argon. (10X)

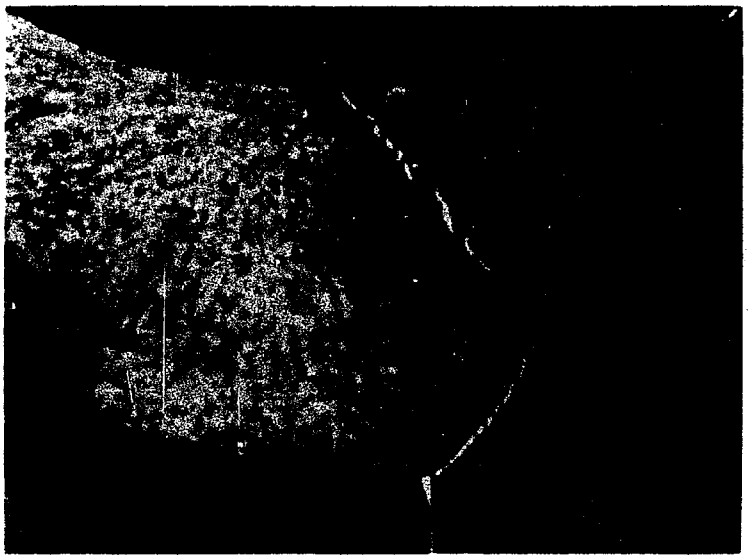

High chemistry HY80, Crack initiated in HAZ

A 212 base metal, Crack initiated in weld metal

Figure 17

Effect of Severity of Restraint on Crack Initiation of Low-Chemistry HY-80

Figure

Effect of Severity of Restraint on Crack Initiation of Low-Chemistry HY80

Lehigh restraint test on 1-inch plate at 250 amperes and 15 inches per minute travel in water saturated argon. (10X)

7" Restraint, 5" Bead, 5" Groove
Crack initiated in HAZ

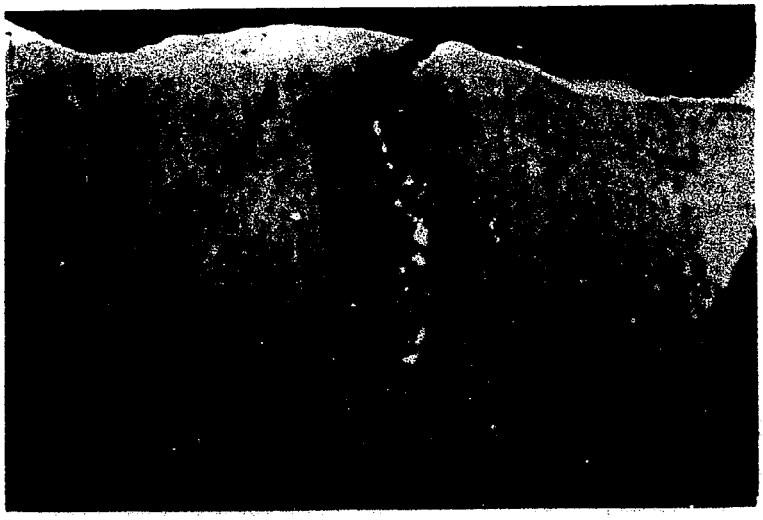

7" Restraint, 3" Bead, 5" Groove
Crack initiated in weld metal

Figure 18

Microcracks

Microcracks

450X, Nital etch
BR22 - weld crack

450X, Unetched
BR22 - weld crack

65X, PR 17, base metal crack, Nital etch. "T-1" steel with triple deox. electrode.

100X, PR 17 **Nital etch**

Figure 19

Comparison of Carbon Equivalent Formulae
Fitted to Cracking Data

COMPARISON OF CARBON EQUIVALENT FORMULAE
FITTED TO CRACKING DATA

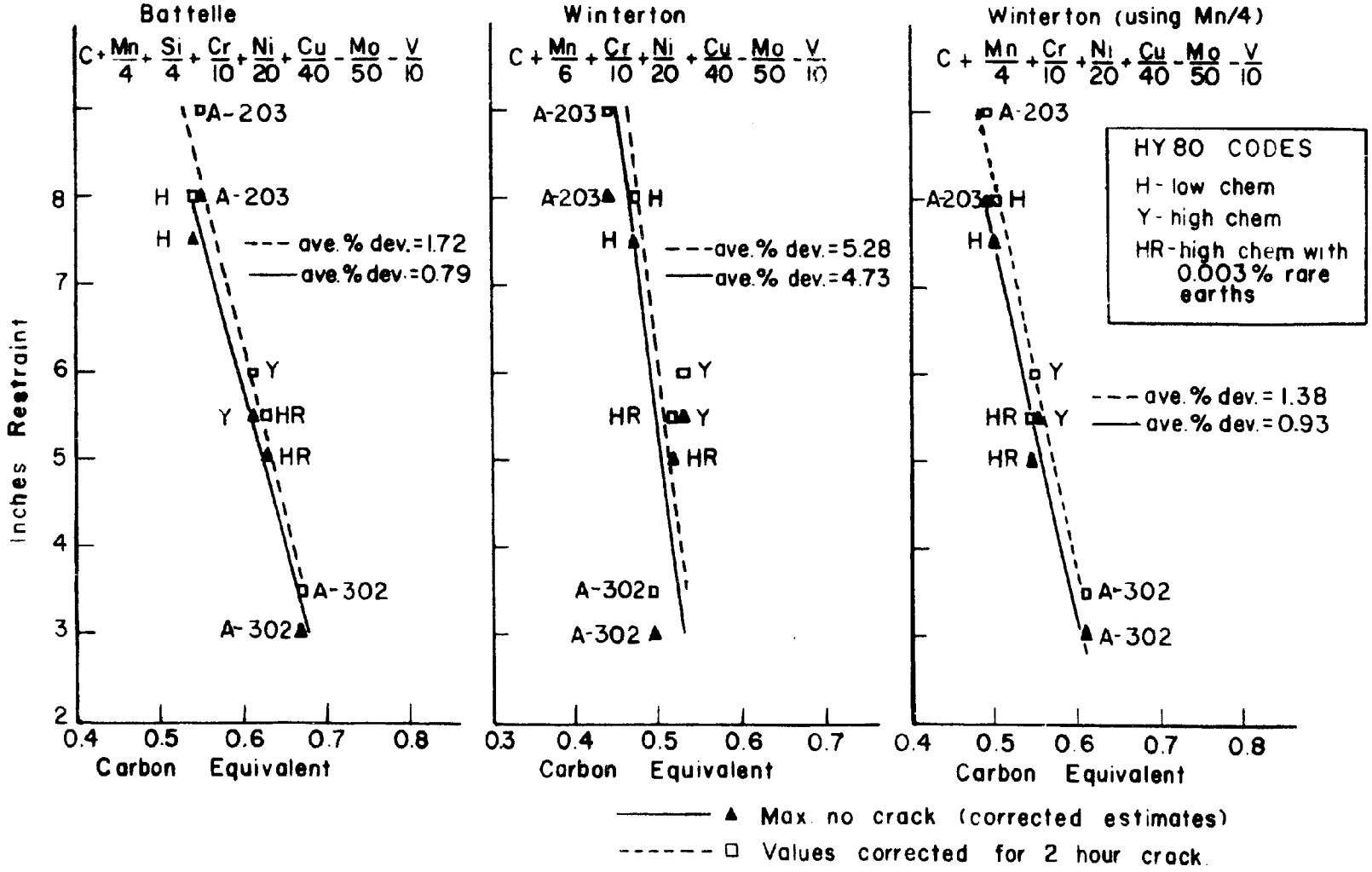

Figure 20

Mathematical Analysis of the Manganese
Factor for the Winterton Formula

MATHEMATICAL ANALYSIS OF THE MANGANESE FACTOR FOR THE WINTERTON FORMULA

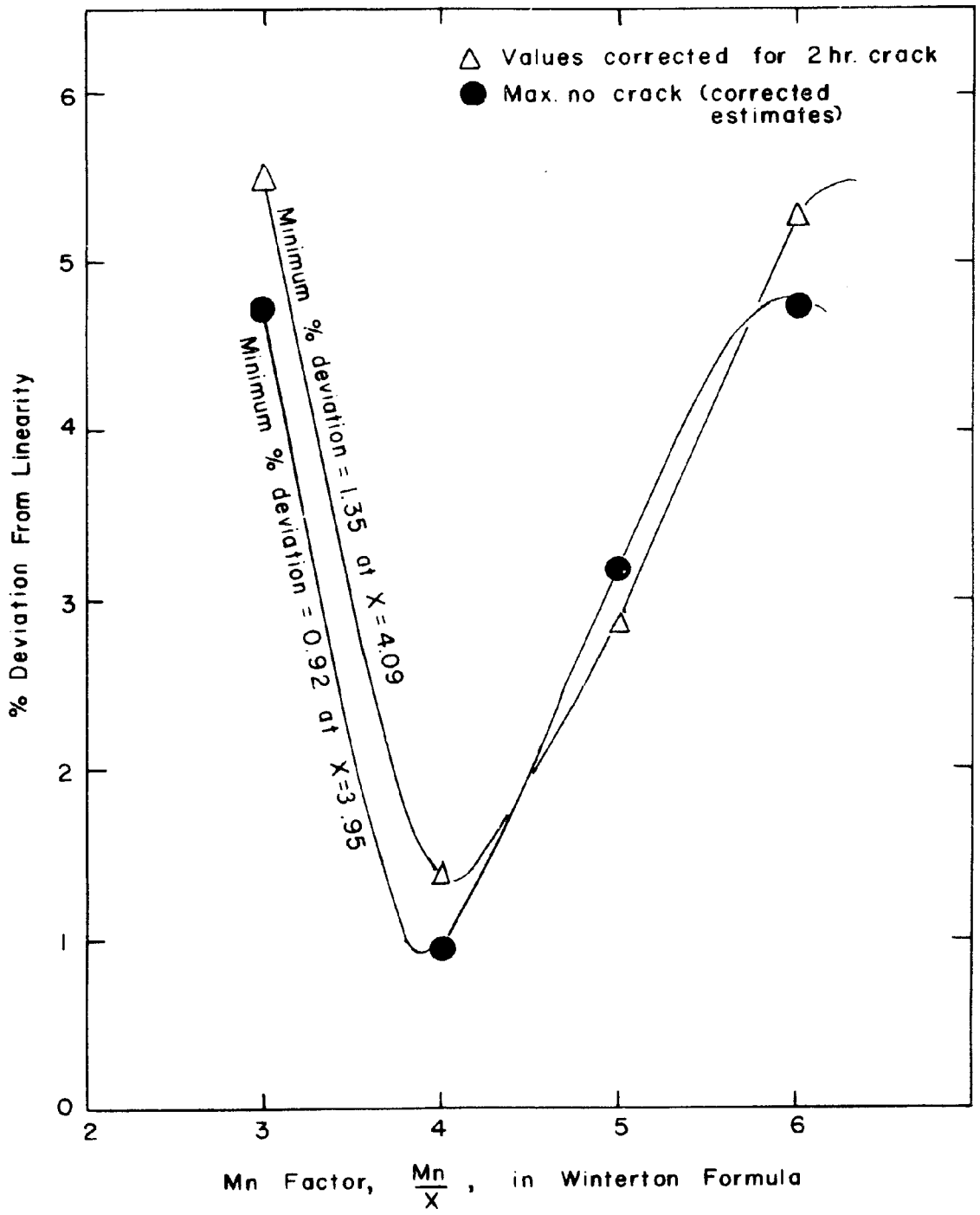

Appendix I - Master Table of Lehigh Restraint Tests

Specimen Code	Welding Conditions Volts, Amps, in/min.	Additions to Argon Atmosphere	Restraint (ins)	Cracking Time (hrs)	Remarks
Navy HY-80 Steel (No. 1), normalized, welded with Alloy No. 2 electrode					
Y3	33, 250, 15	1% H_2O	7	0.41	
Y1	33, 250, 15	"	6	2.5	
Y16	34, 250, 15	"	6	no crack	(120°F preheat)
Y1D	34, 245, 15	"	5	no crack	
Y27	34, 245, 15	"	6	2.2 - 3.0	(slow crack)
Y	--, 250, 15	dry argon	8 (3" groove)	no crack	
Y10	32, 250, 15	1% H_2O	6	18.0	(0°F postcool)
Y13	32, 250, 15	"	6	10.7	(" ")
Y2D	35, 240, 15	"	6	1.5	(150°F postheat)
Y11	34, 250, 15	"	6	no crack	(" ")
Y17	33, 250, 15	"	6	no crack	(" ")
Y22	34, 250, 15	"	6	1.5	double pass, wet-wet
	32, 260, 15	"			
Y12	34, 250, 15	"	5	7.0	double pass, wet-wet
	33, 250, 15	"			
Y26	32, 250, 15	"	4	no crack	double pass, wet-wet
	32, 260, 15	"			
Y21	35, 250, 15	1% H_2O	6	48	double pass, wet-dry
	28, 290, 15	dry argon			
Y25	33, 250, 15	1% H_2O	6	no crack	double pass, wet-dry
	--, 275, 15	dry argon			
Y28	33, 250, 15	dry argon	6	no crack	double pass, dry-wet
	33, 250, 15	1% H_2O			
Y2	--, 250, 15	dry argon	7	no crack	double pass, dry-wet
	--, 250, 15	1% H_2O			
Y20	--, 250, 15	dry argon	8	6.5	double pass, dry-wet
	--, 250, 15	1% H_2O			

Appendix I (Continued)

Specimen Code	Electrode	Welding Conditions Volts, Amps, in/min.	Additions to Argon Atmosphere	Restraint (ins)	Cracking Time (hrs)	Remarks
Navy HY-80 Steel (No. 2)						
HA2	E7016	23, 190, 7.7		6	no crack	normalized plate
HB1	"	22, 215, 8.5		7	" "	" "
HL1	"	22, 200, 7.7		8	" "	" "
HO1	"	22, 200, 7.7		8	2.1-12.1	" "
HD1	"	22, 200, 7.7		8(3" bead)	7.9-14.3	" "
HA1	E9015	22, 200, 7.7		6	no crack	" "
HG2	"	22, 200, 7.7		8	2.0	" "
HZ1	"	22, 200, 7.7		8	0.7	annealed "
HJ2	E6010	27, 180, 8.5		4	no crack	normalized "
HO2	"	27, 180, 8.5		5	" "	" "
HT2	"	27, 180, 8.5		5-1/2	1.0	" "
HK1	"	27, 180, 8.5		6	0.3	" "
HL2	E9010	27, 180, 8.5		5	no crack	" "
HE2	"	27, 180, 8.5		6	0.3	" "
HW2A	"	27, 180, 8.5		5-1/2	no crack	annealed "
HY2	"	27, 180, 8.5		6	4-8	" "
HV2A	"	27, 180, 8.5		6-1/2	0.15	" "
HG1	Alloy 2	33, 320, 19	dry argon	8	no crack	normalized "
HR2	"	32, 250, 15	5% H_2	5	no crack	" "
HN1	"	34, 250, 15	5% H_2	6	1.5	" "
HK2	"	34, 240, 15	"	7	0.6	" "
HF2	"	34, 240, 15	"	8	0.34	" "
HC2	"	34, 250, 15	"	8(3" bead)	0.15	"
HQ1	"	33, 240, 15	1% H_2O	8	2.3	" , DCRP-spray
HJ2	"	35, 240, 15	" "	7	no crack	" " "
HC3	"	28, 190, 10	"	8(3" bead)	0.95	" " drop
HB3	"	--, 195, 10	"	8	no crack	" " "
HM1	"	31, 250, 15	"	5-1/2	" "	" , DCSP-drop
HT1	"	29, 260, 15	"	6-1/2	" "	" " "
HU1	"	29, 250, 15	"	7	" "	" " "

Appendix I (Continued)

Specimen Code	Electrode	Welding Conditions Volts, Amps, in/min.	Additions to Argon Atmosphere	Restraint (ins)	Cracking Time (hrs)	Remarks
HQ1	Alloy 2	32, 250, 15	1% H_2O	8	0.2	normalized, DCRP-spray
HD2	"	35, 240, 15	"	5	no crack	" " "
HB1	"	37, 245, 15	"	5-1/2	" "	"
HS2	"	37, 250, 15	"	6	0.70	"
HH2	"	36, 240, 15	"	7	0.22	"
SQHA1	"	34, 240, 15	"	8	3.0	spheroidized plate
SQHC2	"	35, 240, 15	"	7	2.6	" "
SQHB2	"	34, 240, 15	"	6	no crack	" "
HYA1	"	32, 230, 15	"	7	1.1	annealed plate
HYA2	"	34, 250, 15	"	6	no crack	" "
QHUB	"	35, 240, 15	"	8	no crack	as-quenched plate
QHUA	"	34, 240, 15	"	7	" "	" "
QHB1	"	33, 250, 15	"	8(3" bead)	0.58	" "
QTH1	"	--, 240, 15	"	8	0.45	quenched & tempered
QTH2	"	32, 250, 15	"	7	no crack	" "
Navy HY-80 Steel (No. 3), normalized						
HR1	Alloy 2	29, 270, 15	1% H_2O	6	0.6	
HR3	"	28, 280, 15	"	5	no crack	
HR	"	--, 250, 15	dry argon	8	no crack	
Navy HY-80 Steel (No. 4), normalized						
HAP6	Alloy 2	--, 250, 15	dry argon	8(3" groove)	no crack	
HAP9	"	--, 250, 15	1% H_2O	8	1.3	
HAP7	"	31, 245, 15	"	7	no crack	
HAP3	"	27, 250, 15	"	6	no crack	

Appendix I (Continued)

Specimen Code	Electrode	Welding Conditions Volts, Amps, in/min.	Additions to Argon Atmosphere	Restraint (ins)	Cracking Time (hrs)	Remarks
Navy HY-80 Steel (No. 5)						
HH(3" gr)	Alloy 2	--, 250, 15	dry argon	8(3" groove)	no crack	normalized plate
HH4	"	34, 250, 15	1% H_2O	6	0.75	" "
HH6	"	32, 260, 15	"	5-1/2	0.51	" "
HH2	"	34, 260, 15	"	5	no crack	" "
HH3	"	28, 250, 15	"	5	" "	" "
HHQT2	"	--, 245, 15	"	6	0.50	spray quenched & tempered
HHQT1	"	--, 250, 15	"	5	no crack	"
HH30	Pure Iron	24, 300, 15	"	8(3" groove)	" "	normalized plate
Navy HY-65 Steel (No. 6), normalized						
GN6	Alloy 2	33, 250, 15	1% H_2O	8(3" bead)	1.77	
GN2	"	33, 250, 15	"	8	no crack	
"T-1" Steel (No. 7), quenched & tempered						
PR50	Pure Iron	24, 300, 15	1% H_2O	8(3" groove)	0.3	
PR32	" "	24, 300, 15	"	8(3" bead)	no crack	
PR33	" "	24, 300, 15	"	8	" "	
PR34	" "	24, 300, 15	"	7	" "	
PR25	" "	24, 300, 15	"	6	" "	
PR27	" "	24, 300, 15	"	5	" "	
PR2	Alloy 1	30, 250, 15	"	8	9.6	
PR28	"	33, 250, 15	"	7	3.0	
PR25	"	33, 255, 15	"	6	13.6	
PR24	"	33, 255, 15	"	5	no crack	

Appendix I (Continued)

Specimen Code	Electrode	Welding Conditions Volts, Amps, in/min.	Additions to Argon Atmosphere	Restraint (ins)	Cracking Time (hrs)	Remarks
PR27	Alloy 3	33, 250, 15	1% H_2O	7	4.95	
PR26	"	33, 250, 15	"	6	1.8	
PR20	"	33, 250, 15	"	5	no crack	
PR28D	Triple Deox.	--, 250, 15	"	5	1.2	
PR17	" "	--, 250, 15	"	4	no crack	
PR26	18% Ni Maraging	35, 250, 15	"	6	0.083	
PR3	Alloy 2	33, 250, 15	"	8(3" bead)	0.23	contaminated elec.
PR4	"	33, 250, 15	"	8	1.1	" "
PR5	"	33, 250, 15	"	7	1.6	" "
PR6	"	34, 245, 15	"	6	3.4	" "
PR8	"	33, 250, 15	"	5	3.8	" "
PR9	"	33, 250, 15	"	4	no crack	" "
PR23	"	33, 250, 15	"	8	3.2	
PR12	"	33, 250, 15	"	8	3.6	
PR15	"	33, 245, 15	"	7	1.34	
PR10	"	33, 250, 15	"	6	8.2	
PR11	"	33, 250, 15	"	5	no crack	
PR1	"	34, 250, 15	"	7	no crack	postheat 157°F oven
PR7	"	33, 250, 15	"	8	2.9	

Appendix I (Continued)

Specimen Code	Welding Conditions	Restraint (ins)	Cracking Time (hrs)	Figure 12 Heating Curve	Remarks
Postheated specimens of "T-1" Steel using Alloy 2 electrode with 1% H_2O atmosphere					
PR15	32, 250, 15	7	1.2	(B)	
PR31	33, 245, 15	7	no crack	(G)	
PR19	32, 260, 15	7	no crack	(F)	
PR39	32, 250, 15	7	7.9	(E)	
PR30	32, 245, 15	7	3.3	(D)	
PR29	--, 250, 15	7	2.25	(C)	
PR40&46	32, 250, 15	7	no crack	(I)	
PR38	32, 240, 15	7	3.43	(H)	
PR48	30, 250, 15	7	7.7	(J)	
PR44B	30, 250, 15	7	5.0	(K)	
PR61	30, 245, 15	7	no crack	(L)	
PR45	32, 250, 15	7	" "	(M)	
PR41	30, 250, 15	7	" "	(N)	
PR70	32, 250, 6	8	8.5	(O)	
PR73	34, 235, 6	8	2.3	(P)	
PR43	32, 250, 6	8	2.8	(Q)	
PR76	33, 245, 6	8	3.25	(R)	
PR71	34, 240, 6	8	3.83	(S)	
PR69	--, 250, 6	8	16.0	(T)	
PR64	31, 250, 6	8	no crack	(U)	
PR65	32, 250, 6	8	6.9	(V)	
PR66	31, 250, 6	8	no crack	(W)	
PR67	--, 250, 6	8	" "	(X)	
PR74	31, 250, 6	8	no crack	not reported	postheat 205 min @ 200°F at 7 min after welding, temperature was 200°F, @ 12 min - 190°F, @ 96 min 205°F, @ 202 min - 206°F and fan cooled starting at 205 min.

Appendix I (Continued)

Specimen Code	Welding Conditions	Restraint (ins)	Cracking Time (hrs)	Figure 12 Heating Curve	Remarks
PR13	33, 250, 15	8	2.1		Postheat ir 126°F oven
PR12	34, 250, 15	8	9.6		Postcool @ 0°F
PR10	32, 255, 15	7	8.3		Postcool @ 0°F
PR14	33, 250, 15	6	18.1		Postcool @ 0°F

Appendix I (Continued)

Specimen Code	Electrode	Welding Conditions Volts, Amps, in/min.	Additions to Argon Atmosphere	Restraint (ins)	Cracking Time (hrs)	Remarks
ASTM A-201 Steel (No. 8), as-rolled						
A201-1	Triple Deox.	31, 250, 6	1% H_2O	8(3" groove)	no crack	
A201-8	" "	31, 250, 15	1% H_2O + 5% H_2	8(3" groove)	no crack	
A201-7	Alloy 2	30, 250, 15	1% H_2O	8(3" groove)	no crack	
A201-10	"	35, 240, 15	1% H_2O + 5% H_2	8(3" groove)	no crack	
A201-3	"	30, 250, 15	1% H_2O + 5% H_2	8(1" groove)	no crack	
ASTM A-203 Steel (No. 9), as-rolled						
ER13	Alloy 2	33, 250, 15	1% H_2O	7	no crack	
ER2	"	33, 250, 15	"	8	no crack	
ER10	"	34, 240, 15	"	8(3" bead)	no crack	
ER6	"	33, 250, 15	"	8(3" bead)	5.6	
ER4	"	33, 250, 15	"	8(3" bead)	0.73	
ASTM A-212 Steel (No. 10), as-rolled						
BR22	Alloy 2	33, 250, 15	1% H_2O	5	no crack	
BR23	"	32, 250, 15	"	6	4.5	
BR7	"	34, 250, 15	"	7	0.76	
BR30	"	33, 250, 15	"	7	2.0	
BR33	"	33, 250, 15	"	8	1.2	
BR25	"	33, 250, 15	"	8	2.6	
BR27	"	34, 250, 15	"	8	4.3	0°F postcool
BR31	"	33, 250, 15	"	7	3.3	0°F postcool
BRd	"	32, 245, 15	"	7	0.62	
BR26	"	34, 250, 15	"	8	0.38	125°F postheat
BR28	"	34, 250, 15	"	7	no crack	" "
BR12	Triple Deox.	30, 260, 15	"	8	no crack	
BR11	" "	32, 260, 15	"	8 (3" bead)	1.0	
BRxx	" "	--, 250, 6	"	8 (3" bead)	12.8	

Appendix I (Continued)

Specimen Code	Electrode	Welding Conditions Volts, Amps, in/min.	Additions to Argon Atmosphere	Restraint (ins)	Cracking Time (hrs)	Remarks
ASTM A-302 Steel (No. 11), as-rolled						
A11	Pure Iron	28, 300, 15	1% H_2O	7	0.23	
A2	" "	28, 300, 15	"	5	0.30	
A41	" "	28, 300, 15	"	4-1/2	0.40	
A13	" "	28, 300, 15	"	4	0.60	
A14	" "	28, 300, 15	"	3	no crack	
A6	Triple Deox.	32, 260, 15	"	5	0.54	
A7	" "	32, 260, 15	"	4	0.53	
A23	" "	33, 250, 15	"	3	7.2	
A15	" "	32, 260, 15	"	2-1/2	no crack	
A18	310-SS	33, 250, 15	"	3	no crack	
A27	"	33, 250, 15	"	4	no crack	
A17	"	33, 250, 15	"	5	no crack	
A5	"	33, 250, 15	"	6	no crack	
A9	"	33, 250, 15	"	7	hot crack	
A8	Alloy 2	33, 255, 15	"	6	0.23	
A4	"	33, 250, 15	"	5	0.23	
A3	"	34, 250, 15	"	4	4.1	
A1	"	33, 250, 15	"	3	no crack	
A52	"	--, 250, 15	"	5	0.20	Postheat in 200°F oven
A40	"	--, 250, 15	"	4	0.25	" "
A50	18% Ni Marage	37, 230, 15	"	4	0.083	
18% Nickel Maraging Steel (No. 12)						
M1	18% Ni Marage	32, 250, 15	1% H_2O + 5% H_2	8(3" gr)	no crack	maraged plate
M2	" "	--, 245, 15	" "	8(3" gr)	no crack	annealed plate
M3	Alloy 2	30, 250, 15	1% H_2O	8	no crack	annealed plate
M4	"	30, 250, 15	1% H_2O + 5% H_2	8(3" gr)	no crack	annealed plate

VITA

Charles Gabriel Michael Interrante, the son of Mr. and Mrs. William Interrante of Norristown, Pennsylvania was born in Norristown, Pennsylvania. Preliminary education was obtained in Holy Savior Parochial School, West Norriton Township School and Eisenhower Senior High School where he was graduated as a member of the National Honor Society in June, 1954. In September, 1954 he entered the Junior College of Valley Forge Military Academy in Wayne, Pennsylvania, where he remained until June, 1955. There he became a member of the junior college scholastic honor society, Phi Theta Kappa, and the recipient of the 1955 Physics Achievement Award at V.F.M.A.

In September, 1955 he entered Lehigh University. In June, 1959 he received the Degree of Bachelor of Science in Metallurgical Engineering from Lehigh University. At that time he was appointed Second Lieutenant in the United States Army Reserve. Charles entered the graduate school of Lehigh University in June, 1959 as a research assistant in the Department of Metallurgical Engineering. In October, 1962 he received the Degree of Master of Science in Metallurgical Engineering from Lehigh University. In March 1963 he was ordered to active duty as a First Lieutenant in the Army of the United States. He is presently stationed at the Frankford Arsenal in Philadelphia, Pennsylvania and is engaged in research at the Pitman-Dunn Laboratories.

Professional affiliations include The American Welding Society, and The American Society for Metals.